

Effective resistance in metric spaces

Robi Bhattacharjee* Alexander Cloninger† Yoav Freund‡ Andreas Oslandsbotn§¶

Abstract

Effective resistance (ER) is an attractive way to interrogate the structure of graphs. It is an alternative to computing the eigenvectors of the graph Laplacian.

One attractive application of ER is to point clouds, i.e. graphs whose vertices correspond to IID samples from a distribution over a metric space. Unfortunately, it was shown that the ER between any two points converges to a trivial quantity that holds no information about the graph’s structure as the size of the sample increases to infinity.

In this study, we show that this trivial solution can be circumvented by considering a region-based ER between pairs of *small regions* rather than pairs of *points* and by *scaling the edge weights* appropriately with respect to the underlying density in each region. By keeping the regions fixed, we show analytically that the region-based ER converges to a non-trivial limit as the number of points increases to infinity. Namely the ER on a metric space. We support our theoretical findings with numerical experiments.

1 Introduction

A fundamental task of data science is to model the structure of point clouds embedded in a high-dimensional ambient space. A common approach to this task is to represent the data as a graph where data points are considered vertices, and neighborhood information on the point cloud is encoded in edges connecting the vertices. The edges are often weighted based on the relative distance between points and are usually restricted to local neighborhoods. For simplicity of the introduction, we assume that an edge connects any two vertices whose distance is at most $\gamma > 0$.¹

Measuring the lengths of paths on such graphs is a key component of many methods that seek to characterize point clouds. In the following, we compare two of the most popular graph metrics used for this purpose:

- **Shortest path** defines the distance between two vertices as the minimal number of edges that must be traversed to get from one vertex to the other. This is the most straightforward and intuitive measure of distance and corresponds to the geodesic distance when the point cloud lies on a differentiable manifold. However, the shortest path is sensitive to noise and the subtraction or addition of single points. It is, therefore, unreliable in the context of random point clouds.
- **Effective resistance (ER)**, also called *commute time* is significantly more stable than the shortest path distance as it considers all possible paths between two points instead of only the shortest.

*Department of Informatics, University of California San Diego, 9500 Gilman Dr, La Jolla, CA 92093, United States

†Department of Mathematics, University of California San Diego, 9500 Gilman Dr, La Jolla, CA 92093, United States

‡Department of Computer Science and Engineering, University of California San Diego, 9500 Gilman Dr, La Jolla, CA 92093, United States

§Department of Informatics, University of Oslo, Problemveien 7, 0315 Oslo, Norway

¶Simula Research Laboratory, Kristian Augusts gate 23, 0164 Oslo, Norway

¹More general definitions of edge weights will be given later.

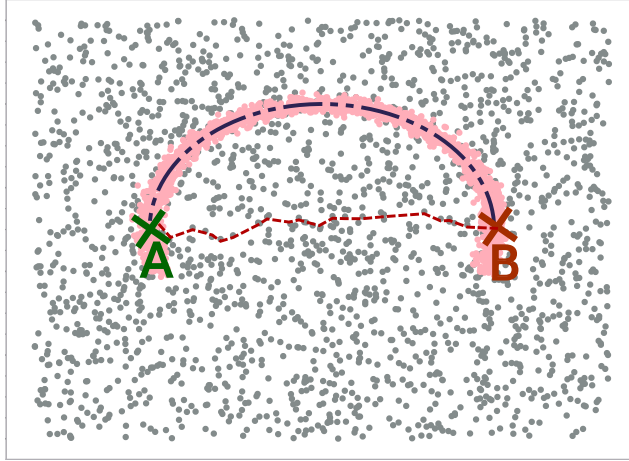


Figure 1: Comparison between ER distance and shortest path distance on a graph constructed on a point cloud. The point cloud consists of a high-density half-moon over a noisy background. The ER distance is the blue dotted line following the half-moon arch. The shortest path distance is the red dotted line across the center of the half-moon.

Specifically, the *hitting time* of vertex B from vertex A is the expected number of edges traversed by a random walk starting at A and ending at B . The *commute time* is the sum of the hitting time from A to B and from B back to A . The *effective resistance* is a metric defined using analogy to resistance networks and is equal to the commute time up to a constant.

Figure 1 shows the difference between the shortest path and the ER distance on a point cloud shaped as a high-density half-moon over a noisy background. The figure illustrates how the shortest path distance would follow the noisy background, while the ER would follow the half-moon arch.

ER has been used in a number of applications in machine learning on topics such as graph sparsification [1], online learning [2], detecting community structure [3] and dimensionality reduction [4]. It has also been used in several other fields ranging from bioinformatics [5] to electronics [6, 7, 8, 9]

A long-standing issue with using ER for point clouds is that the ER distance between points converges to a trivial limit as the number of sampled points increases. This problem has been described in a long line of works [10, 11, 12, 13, 14]. The problem is that in the large graph limit, the ER between two points A and B depends only on the degree (number of neighbors) of A and B . This means that ER distances are not useful for the analysis of the shape of point clouds.

The trivial limit can be described as follows:

Problem 1 (Von-Luxburg limit). *The ER between two nodes i, j in a graph converges as the number of nodes in the graph increases to $1/d_i + 1/d_j$, where d_i, d_j are the degrees of respectively node i and j .*

While the statement of the problem is asymptotic, Von-Luxburg et al. [14] shows that the asymptotic behavior begins already for moderately sized graphs, with the number of nodes in the order of 1000. Moreover, for increasing dimension of the embedding space, this convergence is even faster.

This study aims to develop a new formulation of ER that does not suffer from Problem 1 and can thereby be used to characterize large point clouds.

The key idea is to consider the RE between small regions, rather than individual points. The number of points in a region scales linearly with the total number of points, which avoids the collapse of the RE in the limit. While this is in principle a simple transformation, some care is required to prove that it works as desired.

Our contributions can be summarized as follows:

- We alleviate the problem described by Von-Luxburg et al. [13] by introducing the concept of a

region-based ER between a source and sink region, combined with an appropriate scaling as the sample size grows.

- We prove the existence and convergence of region-based ER to a non-trivial limit.
- We prove that region-based ER is a distance metric. In particular, region-based ER satisfies the triangle inequality.
- We support our theoretical findings with several numerical experiments.

The remainder of this paper is organized as follows. In Section 2, we introduce the concept of a resistor graph, the standard definition of ER, and the definition of ER between sets. In Section 3, we introduce the concept of a metric graph and extend the concept of effective resistance to metric spaces. In Section 4, we show how a finite sample region-based ER converges, with the appropriate scaling, to the limit object region-based ER on a metric space. We provide further results for the region-based ER in Section 5, where we show that it corresponds to the ER between sets and is a distance metric. Meanwhile, Section 6 describes a strategy to control the computational complexity of the ER calculation, using an ε -cover combined with a suitable scaling of the graph weights. Finally, section 7 provide several numerical experiments supporting our theoretical findings.

1.1 Related work

In our work, we show that our region-based ER can be thought of as ER between sets. An extension of the ER to ER between disjoint sets was introduced in Song et al. [15] for application on signed graphs. Song et al. [15] showed that ER between sets is a convex function of the edge weights. Furthermore, it was established that effective resistance between disjoint sets is monotonically increasing w.r.t. decreasing set size. Our contribution is to show that ER between sets can be generalized to ER over a metric space. We prove convergence to a non-trivial limit as the graph size increases and give numerical evidence that this limit is meaningful. Furthermore, we prove the triangle inequality and show that region-based ER is a distance metric.

2 Resistor Graphs

In this section, we review several key ideas and concepts about *resistor graphs* and the effective resistance. Finally, we introduce the notion of effective resistance between sets.

We start by formulating our setting. Let $G = (X, W)$ be an un-directed, weighted graph with nodes $X = \{x_1, \dots, x_n\}$, and edge weights $W_{i,j}$ and let $L = D - W$ be the graph Laplacian, where D is the degree matrix $D_{ii} = \sum_j W_{ij}$.

The graph can be thought of as an electrical network where each edge (x_i, x_j) has a non-negative *resistance* $R(x_i, x_j) = 1/W_{ij}$. With further analogy to electrical circuits, we can interpret a function $v : X \rightarrow \mathbb{R}$ on the graph's vertices as a voltage $v(x_i)$ and assign to each edge a signed *current* $J_{i,j} = -J_{j,i}$, which can be related to the resistance and voltages through Ohm's law. The relation can be written as

$$v(x_i) - v(x_j) = R(x_i, x_j)J_{i,j} \quad \text{or alternatively} \quad J_{i,j} = W_{ij}(v(x_i) - v(x_j)). \quad (2.1)$$

Meanwhile, from Kirchhoff's law, the sum of currents entering a node i must be zero, namely

$$\sum_{j \sim i} J_{i,j} = J_{ext,i}, \quad (2.2)$$

where $J_{ext,i}$ is an external current that can be either a source, a sink, or zero if the node is unconstrained (no external source applied). Combining these laws, we have that

$$(Lv)_i = \sum_{j \sim i} W_{ij}(v(x_i) - v(x_j)) = J_{ext,i} \quad (2.3)$$

Furthermore, since energy transfer in an electrical circuit is voltage times charge. We can define the *energy* of the voltage v as

$$E(v) \doteq \sum_{x_i, x_j \in X} W_{i,j} (v(x_i) - v(x_j))^2 = v^T L v \quad (2.4)$$

2.1 Effective resistance

The ER is a measure for calculating distances on graphs [16], which considers all possible paths between two nodes, as opposed to the shortest-path metric. As such, the ER captures the graph's structure more carefully, which can be advantageous in many applications. Using the analogy to electrical circuits, effective resistance can be defined in two equivalent ways based on $R(x_i, x_j) = \Delta V / J$, where ΔV is the voltage difference and J the total current flowing between the two nodes. In the **voltage difference formulation**, the current flow is constrained to unity, and the resistance is given in terms of the voltage difference between the nodes. In the **current flow formulation** the voltage difference is constrained to unity, and the resistance is given in terms of the inverse of the total current flow between the nodes. The following definitions formalize these approaches.

Definition 2.1 (Effective resistance (voltage difference formulation)). *The effective resistance $R(x_i, x_j)$ between two nodes $x_i, x_j \in X$ in a graph is the voltage difference between the nodes when a current of one ampere is injected between the source node x_i and extracted from the sink node x_j .*

Definition 2.2 (Effective resistance (current flow formulation)). *The effective resistance $R(x_i, x_j)$ between two nodes $x_i, x_j \in X$ in a graph is the inverse of the current flow between the nodes with the boundary conditions $v(x_i) = 1$ and $v(x_j) = 0$.*

From Definitions 2.1 and 2.2, we know that $R(x_i, x_j)$ can be found from the voltage or current in the system when the other is appropriately constrained. However, we still need a way to explicitly calculate these quantities. Several approaches exist for calculating the ER, and a summary of different formulations can be found in Theorem 4.2 in Jørgensen and Erin [17]. However, in this work we restrict ourselves to the two formulations that follow most naturally from Definitions 2.1 and 2.2 respectively.

Proposition 2.3 (Voltage difference formulation). *The effective resistance between nodes x_i, x_j corresponds to $R(x_i, x_j) = v(x_i) - v(x_j) = E_{min}$, where v is the function that minimizes the energy*

$$\begin{aligned} \min_v \quad & \sum_{x_i, x_j \in X} W_{i,j} (v(x_i) - v(x_j))^2 \\ \text{Subject to} \quad & (Lv)_i = 1, \quad (Lv)_j = -1, \quad (Lv)_i = 0, \forall i \in X \setminus \{x_i, x_j\} \end{aligned}$$

Proof. See Theorem 4.2, Jørgensen and Erin [17]. □

Proposition 2.4 (Current flow formulation). *The effective resistance between nodes x_i, x_j corresponds to $R(x_i, x_j) = 1/J_{tot}$, where*

$$J_{tot} = \sum_{j \in X} W_{i,j} (v(i) - v(j))$$

and v is the function that minimizes the Dirichlet energy

$$\begin{aligned} \min_v \quad & \sum_{x_i, x_j \in X} W_{i,j} (v(x_i) - v(x_j))^2 \\ \text{Subject to} \quad & v(x_i) = 1, \quad v(x_j) = 0 \end{aligned}$$

Proof. See Theorem 4.2, in Jørgensen and Erin [17]. □

We note that the standard formulation of effective resistance

$$R(x_i, x_j) = (e_i - e_j)^\top L^\dagger (e_i - e_j)$$

can easily be derived from $R(x_i, x_j) = v(x_i) - v(x_j) = (e_i - e_j)^\top v$ and the constraints $Lv = e_i - e_j$ in Proposition 2.3, which gives $v = L^\dagger(e_i - e_j)$. This relation shows how ER is an euclidean distance matrix [18]. Furthermore, it show how the distance between nodes using ER, can be computed without explicitly calculating the voltage functions v . Instead, it suffices to solve for L^\dagger , the pseudo-inverse of L . Methods have also been proposed for distributed computation [19].

Lemma 2.5. *Effective resistance satisfies the triangle inequality and is a distance metric on graphs*

Proof. See e.g. Jørgensen and Erin [17], Ghosh et al. [18] or Klein and Randić[16]. \square

Remark 2.6. *We note that the **voltage difference formulation** corresponds to a Poisson problem since the constraints on the current are applied as an inhomogenous term on the Laplace equation $Lv = e_1 - e_2$. Similarly, the **current flow formulation** corresponds to a Dirichlet problem since it solves a homogenous Laplace equation with the constraints applied as boundary conditions.*

2.2 Effective Resistance Between Sets

In this study, we propose considering the ER between small regions rather than pairs of points to achieve a non-trivial limit in the metric graph setting. Our first step in this regard is to extend the concept of effective resistance to effective resistance between sets. Whereby sets, we mean subsets of the graph nodes X . The effective resistance between sets was defined in Definition 2 [15], in terms of the Schur complement of the Laplacian. For the analysis in this paper, we consider the current flow interpretation from Song et al. [15] and use this to write down an equivalent formulation that generalizes the current flow formulation from Proposition 2.4 to the effective resistance between sets. We consider the sets $X_a, X_b \subset X$ and $X_c = X \setminus (X_a \cup X_b \cup X_z)$ and let $R^s(X_a, X_b)$, defined in Definition 2.7, denote the effective resistance between two sets. Proposition 2.8 tells us how we can explicitly calculate $R^s(X_a, X_b)$.

Definition 2.7 (Effective resistance between sets (current flow formulation)). *The effective resistance $R^s(X_a, X_b)$ between two non-empty disjoint sets $X_a, X_b \subset X$ in a graph is the inverse of the current flow between the two subsets with the boundary conditions $v(x_i) = 1, \forall i \in X_a$ and $v(x_i) = 0, \forall i \in X_b$.*

Proposition 2.8 (Current flow formulation on sets). *The effective resistance between the non empty disjoint subsets $X_s, X_g \subset X$ corresponds to $R^s(X_s, X_g) = 1/J_{tot}$, where*

$$J_{tot} = \sum_{i \in X_s} \sum_{j \in X} W_{ij} (v(i) - v(j))$$

and v is the function that minimizes the energy

$$\begin{aligned} \min_v \quad & \sum_{x_i, x_j \in X} W_{i,j} (v(x_i) - v(x_j))^2 \\ \text{Subject to} \quad & v(x_i) = 1 \forall i \in X_s, \quad v(x_i) = 0, \forall i \in X_g \end{aligned}$$

Proof. Definition 2 and Theorem 1 in Song et al. [15]. \square

3 Effective Resistance over metric spaces

Our goal is to extend the concept of effective resistance to metric spaces. To this end, we start by defining a particular type of graph, namely graphs constructed from samples drawn from a distribution over a metric space. Let (M, d) be a compact metric space and μ , a probability measure over M .

Let $k : M \times M \rightarrow [0, 1]$ be a kernel function that defines what it means for two points to be "near" each other. Commonly used kernel functions are:

- The radial kernel: $k_r(x, y) = \mathbb{1}(d(x, y) \leq r)$ where $r > 0$ is some fixed radius.
- The Gaussian kernel: $k_\sigma(x, y) = \exp(\frac{-d(x, y)^2}{2\sigma^2})$, where $\sigma > 0$ is the fixed temperature parameter.

Next, let $M_s \subseteq M$ and $M_g \subseteq M$ be two disjoint measurable subsets of M . As before, we let $k : M \times M \rightarrow [0, 1]$ be a kernel function.

To define the effective resistance between M_s and M_g , we begin by defining the energy-minimizing voltage induced by μ and k over these sets.

Definition 3.1. Let $M_s, M_g \subseteq M$ be measurable disjoint subsets, k a kernel function, and μ a probability measure over M . Let V_{M_s, M_g} be the set of all measurable functions $v : M \rightarrow [0, 1]$ with $v(x) = 1$ for all $x \in M_s$ and $v(x) = 0$ for all $x \in M_g$. For any such v , define its energy as

$$E(v) = \int_M \int_M k(x, y)(v(x) - v(y))^2 d\mu(x)d\mu(y).$$

Then we say that $v^* \in V_{M_s, M_g}$ is an energy minimizing voltage if it is a global minimum of $E(v)$, meaning that

$$v^* = \operatorname{argmin}_{v \in V_{M_s, M_g}} E(v).$$

Observe that Definition 3.1 does not necessarily imply a unique energy minimizing voltage induced by M_s and M_g . However, under certain technical conditions on k, μ , and M , we can show that uniqueness holds, which will be crucial for defining the effective resistance between M_s and M_g .

3.1 Technical conditions of M , μ , and k

We begin with the notion of a normalized kernel, which integrates to 1 over any fixed point $x \in M$.

Definition 3.2. The normalized kernel of k , denoted $\hat{k} : M \times M \rightarrow R$, is defined as

$$\hat{k}(x, y) = \frac{k(x, y)}{\int_M k(x, z)d\mu(z)}.$$

A normalized kernel can be thought of as the natural analog of a degree normalized weight matrix. We can easily verify that $\int \hat{k}(x, y)d\mu(y) = 1$ for all x .

Next, we generalize the notion of *adjacency* to the metric setting.

Definition 3.3. Let $A \subseteq M$ a measurable set and $\alpha > 0$. Define $C_\alpha(A)$ as the set of all x such that $\int_A \hat{k}(x, y)d\mu(y) > \alpha$.

$C_\alpha(A)$ can be thought of as a continuous generalization of the set of “neighbors” of A . In the finite setting $C(A)$ would comprise of vertices that are adjacent to some vertex in A . The parameter α provides a lower bound on the degree of connectivity.

Next, we continue this to develop an analogous generalization of vertices that are path connected to A . To do so, we first define the convolution operation over kernel similarity functions.

Definition 3.4. Let p, q be kernel functions $p : M \times M \rightarrow [0, 1]$, $q : M \times M \rightarrow [0, 1]$. Then their convolution is the function $p \circ q : M \times M \rightarrow [0, 1]$ defined by

$$(p \circ q)(x, y) = \int_M p(x, z)q(z, y)d\mu(z).$$

We let $p^{(i)}$ denote $p \circ p \circ \dots \circ p$ repeated i times.

The key idea is that the kernel $\hat{k}^{(i)}$ corresponds to paths of length i . As a result, we now define C_α^i accordingly.

Definition 3.5. Let $A \subseteq M$ a measurable set. Then $C_\alpha^i(A)$ denotes the set of all x for which $\int_A \hat{k}^{(i)}(x, y) d\mu(y) \geq \alpha$.

We will now restrict our interest to metric spaces M for which $M = C_\alpha^m(A)$ for some fixed integer $m > 0$, and real number $\alpha > 0$. This condition essentially means that the graphs we consider are both path connected and have bounded diameter, and the parameter α implies that this connection has a degree of robustness. We note that these assumptions are extremely mild: for example, any compact manifold using a radial or Gaussian kernel can be easily shown to satisfy them.

3.2 Defining the effective resistance

We now show that under the previously discussed technical conditions, there exists a unique energy minimizing voltage with respect to M_s, M_g, k , and μ .

Proposition 3.6. Let k be a kernel, M , a metric space, and μ a measure over M . Let M_s and M_g be measurable disjoint subsets of M . Suppose there exists $\alpha > 0$, $m > 0$ such that $M = C_\alpha^m(M_g \cup M_s)$ (Definition 3.5). Then for any measurable disjoint sets M_s and M_g , there exists a unique energy minimizing voltage v^* (Definition 3.1) over M with M_s as its source and M_g as its sink.

Given a unique energy-minimizing voltage, we can then define the effective resistance between M_s and M_g as the inverse of the induced current between them by v^* .

Definition 3.7 (Effective resistance on metric space). Let M_s, M_g be non-empty measurable disjoint subsets of M such that they have a unique energy minimizing voltage, v^* , with respect to measure μ and kernel k . Then their effective resistance is defined as $R^\mu(M_s, M_g) = 1/J_{tot}$, where

$$J_{tot} = \int_{M_s} \int_M k(x, y)(v^*(x) - v^*(y)) d\mu(x) d\mu(y).$$

4 Convergence towards the effective resistance

In this section, we show how the effective resistance between two subsets of metric space M , M_s , and M_g , can be approximated by computing the effective resistance of a graph induced by points sampled from the probability measure, μ , over M . To this end, let $X_n = \{x_1, x_2, \dots, x_n\} \sim \mu$ be a set of points sampled from data distribution μ over M . Using one of the kernels defined above, a weighted graph can be constructed on the samples by assigning weights $W_{ij} \propto k(x_i, x_j)$ between each pair of points $x_i, x_j \in X_n$.

Definition 4.1 (Metric resistor graph). Let X_n a sample as defined above and $k : M \times M \rightarrow [0, 1]$ be a kernel similarity function. Then the **metric resistor graph**, $G_n = (X_n, W)$, is the weighted graph with edge weights $W_{ij} = \frac{k(x_i, x_j)}{n^2}$.

In the next section, we take a closer look at the scaling factor $1/n^2$.

4.1 Scaling

Our goal is to construct a definition of the effective resistance that converges towards a non-trivial solution as the number of sampled points, n , goes towards infinity. To achieve this, it is necessary that the edge weights W_{ij} scale appropriately with the number of samples. It is natural to demand that the physical properties of the graph, embodied by the resistance, current, and voltage, should remain relatively stable as n increases. Thus, it is crucial to understand how the edge resistances should scale with the number of points sampled.

Intuition To this end, consider two small regions T and T' such that $k(x, x') > 0$ for all $x \in T$ and $x' \in T'$. For simplicity, let $k(x, x')$ be constant, which means each edge has equal resistance $R = 1/k(x, x')$. We aim to keep the resistance between these two regions constant as the number of points changes. For a fixed X_n , on average there are m points $x \in S_n = \{x \in X_n : x \in T\}$ and m points $x' \in S'_n = \{x \in X_n : x \in T'\}$. This results in m^2 edges between T and T' . This means the total resistance between these regions is R/m^2 , given that these edges are connected in parallel.

The issue here is that, once we move to a denser sample X_{2n} , there will be, on average, $2m$ points in S_{2n} and S'_{2n} respectively. This will create a net resistance $\frac{1}{4}R/m^2$, which means the resistance between these physical regions T, T' decreases and will go to 0 as n goes to infinity. We illustrate this construction in Figure 2.

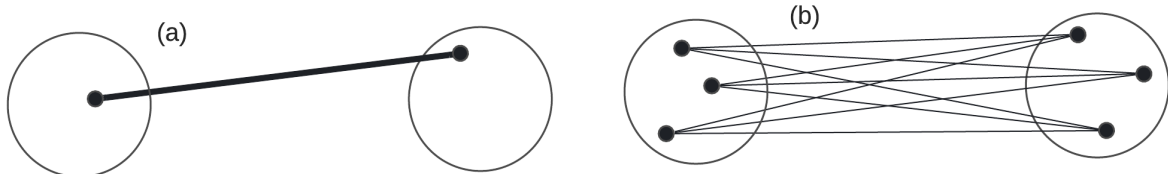


Figure 2: Example of resistance scaling. **(a)** Number of edges connecting T and T' for $m = 1$ point sampled from each region. **(b)** Number of edges connecting T and T' for $m = 3$ points sampled from each region. Notice that the number of edges between these regions is m^2 .

Point-wise scaling In order to overcome this issue of decreasing net resistance, we introduce a point-wise scaling $\gamma_{ij} = 1/n^2$ for all node pairs i, j , to compensate for the m^2 factor. Here $m = pn$ where p is the probability that a sample drawn from X_n falls in region T . In other words, with the point-wise scaling, we have the net resistance $\frac{1}{4}R/pp'$, where p, p' are constant with respect to n .

Having defined the proper scaling, we now define the random object, v_n^* , which is the energy-minimizing voltage induced by a metric graph constructed from an i.i.d sample of n points from M .

Definition 4.2 (Energy minimizing voltage over metric graph). Let M_s, M_g be disjoint measurable sets in M . For $X_n \sim \mu^n$, let $v_{X_n} : X_n \rightarrow [0, 1]$ be defined as the energy minimizing voltage over the metric graph G_n where the weights W_{ij} are defined by $W_{ij} = \frac{1}{n^2}k(x_i, x_j)$. Then $v_n^* : M \rightarrow [0, 1]$ denotes the function

$$v_n^*(x) = \begin{cases} 1 & x \in M_s \\ 0 & x \in M_g \\ \frac{\sum_{x_i \in X_n} k(x, x_i) v_{X_n}(x_i)}{\sum_{x_i \in X_n} k(x, x_i)} & x \in M \setminus (M_s \cup M_g) \end{cases}.$$

Note that v_n^* represents a random variable over functions $M \rightarrow [0, 1]$ with randomness induced by the randomness of X_n .

We similarly define the region-based ER, $R_n(M_s, M_g)$ as follows.

Definition 4.3 (Region-based effective resistance). Let M_s, M_g be disjoint measurable sets in M . For $X_n \sim \mu^n$, let v_n^* be defined as the energy minimizing voltage over the metric graph, G_n where the weights W_{ij} are defined by $W_{ij} = \frac{1}{n^2}k(x_i, x_j)$. We then define the region-based ER $R_n(M_s, M_g) = 1/J_{tot}$ where J_{tot} is as defined in Proposition 2.8 with the voltage v_n^* . Note that $R_n(M_s, M_g)$ corresponds to a random variable, denoted R_{X_n} , induced by the randomness of X_n .

4.2 Convergence analysis

We now show that the finite sample energy minimizing voltage, v_n^* , and the finite sample region-based ER, $R_n(M_s, M_g)$, converge towards the limit objects v^* and $R^\mu(M_s, M_g)$.

Theorem 4.4. *Let M, k , and μ satisfy that there exists $m > 0$ and $\alpha > 0$ such that $M = C_\alpha^m(M_g \cup M_s)$. Let M_s, M_g be disjoint measurable subsets of M , and let $v_n^*, v^*, R_n(M_s, M_g)$, and $R^\mu(M_s, M_g)$ be as defined in Definitions 4.2, 3.1, 4.3, and 3.7. Then the following hold:*

1. *For any $x \in M$, the sequence $v_1^*(x), v_2^*(x), \dots$ converges to $v^*(x)$ in probability.*
2. *The sequence $R_1(M_s, M_g), R_2(M_s, M_g), \dots$ converges to $R^\mu(M_s, M_g)$ in probability.*

A proof can be found in Appendix B.

5 Properties of the effective resistance between sets

We have established that the finite sample region-based ER $R_n(M_s, M_g)$ from Definition 4.3 converges to the ER on a metric space $R^\mu(M_s, M_g)$, defined in Definition 3.7. In this section, we establish that $R_n(M_s, M_g)$ is a distance metric. In particular, we prove that it satisfies the triangle inequality.

Consider a metric space M and a sample $X_n \sim \mu^n(M)$. For two disjoint measurable subsets $M_s, M_g \subset M$ we can denote the corresponding subsets of X_n as $X_s = \{x \in X_n : x \in M_s\}$ and $X_g = \{x \in X_n : x \in M_g\}$. The region-based ER $R_n(X_s, X_g)$ over a finite sample can be thought of as the ER between sets, namely $R^s(X_s, X_g)$ as defined in Section 2.2. For the analysis in this section, this is the interpretation we will take.

In the following, we will introduce the subscript G on $R_G^s(X_a, X_b)$ to indicate the graph over which the ER is calculated. From Lemma E.3 it follows that $R_G^s(X_a, X_b) = R_{G_{ab}}^s(a, b) = (e_1 - e_2)^\top L_{G_{ab}}^\dagger (e_1 - e_2)$ where $L_{G_{ab}}$ is the Laplacian on the reduced graph G_{ab} defined in Definition E.1. Symmetry and positive semi-definiteness of $R_G^s(X_a, X_b)$ follows therefore from the classical result on the reduced graph G_{ab} [17, 18, 16].

Meanwhile, the triangle inequality is established by Theorem 5.1.

Theorem 5.1. *(Triangle inequality for effective resistance between sets) Consider a graph $G = (X, W)$ and the non-empty disjoint subsets $X_a, X_b, X_z \in X$. Let $R^s(X_p, X_q)$ be the ER between sets X_p, X_q for $p, q \in \{a, b, z\}$. We then have*

$$R^s(X_a, X_b) \leq R^s(X_a, X_z) + R^s(X_z, X_b)$$

Proof. Appendix E.2. □

Having established the triangle inequality along with symmetry and positive semi-definiteness, it follows that the effective resistance between disjoint sets is a distance metric.

6 Computational considerations

In practice, calculating the effective resistance in the large graph limit is not computationally viable. This is because the computational cost directly increases with n , the number of sampled points. For large values of n , it can be relatively expensive to compute the effective resistance – especially if we desire to do so for many pairs of regions M_s, M_g . To control the computational complexity of the calculation, we suggest building the graph on a partitioning of the data which we call an α -cover \mathcal{C} to remove the dependency on n . Furthermore, in order to incorporate information about the density, we combine the α -cover with a suitable scaling of the graph weights.

6.1 Alpha-cover

Let (M, d) be a metric space and consider an α -cover \mathcal{C} as defined in Definition 6.1. The α -cover is closely related to the concept of doubling dimension $\text{ddim}(M)$ as defined in Definition A.1, which is a measure of the intrinsic dimension of M . In fact, if $\mathcal{B}(\eta)$ is the smallest ball such that $M \subseteq \mathcal{B}(\eta)$ and $\alpha = 2^{-\ell}\eta$, then it follows that $|\mathcal{C}| = 2^{\ell \text{ddim}(M)}$. This means that the size of the α -cover depends only on the resolution, span of the data, and the intrinsic dimension of M , while it is independent of n .

Definition 6.1 (α -cover). Let (M, d) be a metric space. A subset $\mathcal{C} \subseteq M$ is an α -cover of M if it satisfies the following two conditions.

1. (Packing property): All points $y_1, y_2 \in \mathcal{C}$ are such that $d(y_1, y_2) \geq \alpha$
2. (Covering property): For all points $x \in M$ there exists $y \in \mathcal{C}$ such that $d(x, y) \leq \alpha$

To construct the α -cover, a popular algorithm is the cover-tree algorithm, see e.g. Beygelzimer et al. [20] and Oslandsbotn et al. [21] (which is the algorithm we use in this paper).

Region-wise scaling In order to incorporate information about the underlying distribution $\mu(M)$, we combine the α -cover with a region-wise scaling as an alternative to the scaling suggested in Section 4.1. This is important because, as mentioned in the introduction, one of the desirable properties of ER is that it can capture cluster structures in graphs, which in turn means information about the underlying data distribution $\mu(M)$. Because this information is lost with the α -cover, due to the uniform partitioning, a scaling that captures the density is necessary.

To formally define this scaling, we first introduce the concept of a Voronoi cell

Definition 6.2 (Voronoi cell). Let \mathcal{C} be an α -cover as defined in Definition 6.1. We define the Voronoi cell associated with point $x_i \in \mathcal{C}$ as

$$\mathcal{V}_i = \{x \in M : d(x_i, x) \leq d(x_j, x) \forall x_i, x_j \in \mathcal{C}\}$$

We can then define the scaling γ_i for a given sample $X_n \sim \mu^n(M)$.

Definition 6.3 (Region-wise scaling). Let X_n be a sample as defined above and \mathcal{C} the associated α -cover. With each center, $x_i \in \mathcal{C}$, we associate a scaling constant

$$\gamma_i = \frac{|\{x \in X_n : x \in \mathcal{V}_i\}|}{n}$$

The interpretation of γ_i is that it is the empirical local probability density associated with each Voronoi cell in the α -cover. It can easily be estimated by counting the number of samples $x \in X_n : x \in \mathcal{V}_i$, divided by the total number of samples n .

Remark 6.4. We note that for the α -cover approach, we can not use the point-wise scaling introduced in Section 4.1. To see this, consider the discussion in Section 4.1, which showed that the net resistance between two regions T and T' is $\frac{1}{4}R/m^2$. For data sampled from μ , it follows that $m \propto n$. However, for the α -cover, we have instead $m \propto |\mathcal{C}|$, and the size of the epsilon cover $|\mathcal{C}|$ depends only on the doubling dimension of the data and not on n .

6.2 Effective resistance on α -cover

Our idea is to construct a graph on the α -cover, instead of directly on X_n , and then define the ER on this graph instead. We call this new graph the Cover resistor graph.

Definition 6.5 (Cover resistor graph). Let \mathcal{C} be an α -cover, and let X_n a sample as defined above and $k : M \times M \rightarrow [0, 1]$ be a kernel similarity function. Let γ_i, γ_j be the region-wise scaling weights defined in Definition 6.3. Then the **cover resistor graph**, $G_n^{\mathcal{C}} = (\mathcal{C}, W)$, is the weighted graph with edge weights $W_{ij} = \gamma_i \gamma_j k(x_i, x_j)$.

The cover resistor graph essentially uses the nodes of the cover as vertices and constructs weights based on the relative *weights* of each cover node.

We now show that computing effective resistance over the cover resistor graphs converges to the same limit object that using the sampled metric graphs in the previous section does. To do so, we begin by defining analogs of v_n^* and $R_n(M_s, M_g)$.

Definition 6.6 (Energy minimizing voltage over α -cover). Let \mathcal{C} be an α -cover, and $G_n^{\mathcal{C}}$ be its cover resistor graph constructed from sample X_n , source and sink regions M_s and M_g , and kernel function k . Let $v_{X_n, \mathcal{C}} : \mathcal{C} \rightarrow [0, 1]$ denote the energy minimizing voltage function over $G_n^{\mathcal{C}}$. Then we let $v_n^{\mathcal{C}} : M \rightarrow [0, 1]$ be defined as

$$v_n^{\mathcal{C}}(x) = \begin{cases} 1 & x \in M_s \\ 0 & x \in M_g \\ \frac{\sum_{c_i \in \mathcal{C}} k(x, c_i) v_{X_n}(x_i)}{\sum_{c_i \in \mathcal{C}} k(x, c_i)} & x \in M \setminus (M_s \cup M_g) \end{cases}.$$

Note that $v_n^{\mathcal{C}}$ represents a random variable over functions $M \rightarrow [0, 1]$ with randomness induced by the randomness of X_n .

Definition 6.7 (Region-based ER on α -cover). Let \mathcal{C} be an α -cover, let $v_n^{\mathcal{C}}$ be the associated energy minimizing voltage and let $G_n^{\mathcal{C}}$ be the cover resistor graph from Definition 6.5 constructed from sample $X_n \sim \mu^n$. Consider the source and sink regions M_s and M_g . We define the region-based ER on the α -cover as $R_n^{\mathcal{C}}(M_s, M_g) = 1/J_{\text{tot}}$ where J_{tot} is as defined in Proposition 2.8 but now with respect the sets $\mathcal{C} \cap M_s, \mathcal{C} \cap M_g$, the graph $G_n^{\mathcal{C}}$ and the voltage $v_n^{\mathcal{C}}$. Note that $R_n^{\mathcal{C}}(M_s, M_g)$ denotes the random variable, $R_{X_n}^{\mathcal{C}}$, induced by the randomness of X_n .

We now show that similarly to v_n^* and $R_n(M_s, M_g)$, for sufficiently small values of α , $v_n^{\mathcal{C}}$ and $R_n^{\mathcal{C}}(M_s, M_g)$ converge to the same quantities.

Theorem 6.8. Let M be a metric space, k a kernel similarity function, and μ be a measure over M . Let M_s and M_g be two disjoint measurable subsets of M such that $M = C_{\beta}^m(M_s \cup M_g)$ for some $m, \beta > 0$. Then there exists a function $\Delta : \mathbb{R}^+ \rightarrow \mathbb{R}^+$ such that the following properties hold. First, $\lim_{\alpha \rightarrow 0^+} \Delta(\alpha) = 0$. Second, for any $\alpha > 0$ and any α -cover of M , \mathcal{C} , the following two conditions hold.

1. For any $x \in M$, the sequence $v_1^{\mathcal{C}}(x), v_2^{\mathcal{C}}(x), \dots$ converges in probability, and satisfies that

$$|\lim_{n \rightarrow \infty} v_n^{\mathcal{C}}(x) - v^*(x)| < \Delta(\alpha).$$

2. The sequence $R_1^{\mathcal{C}}(M_s, M_g), R_2^{\mathcal{C}}(M_s, M_g), \dots$ converges in probability and satisfies that

$$|\lim_{n \rightarrow \infty} R_n^{\mathcal{C}}(M_s, M_g) - R^{\mu}(M_s, M_g)| < \Delta(\alpha).$$

This result implies that for a sufficiently small value of α , we can essentially replace our sample X_n with any α -cover, \mathcal{C} , of M .

6.3 A note on the advantages of using an α -cover

The advantages of defining the ER on an α -cover are two-fold:

1. With the α -cover, the size of the graph and, therefore, the computational complexity of computing the ER can be controlled independently of n .
2. The approximation of the density can be refined in a continuous manner by updating the local probabilities using more samples from $\mu(M)$, without the need to change the size of the graph.

For example, with $\alpha = 2^{-l}\eta$, it follows that $|\mathcal{C}|$ and, therefore, the graph size grows as $\mathcal{O}((\eta/\alpha)^{\text{ddim}(M)})$. This means that the size of the α -cover depends only on the resolution we want α , the span of the data η , and the doubling dimension $\text{ddim}(M)$ of M (Definition A.1).

We note that the α -cover, with region-wise scaling, satisfies the criteria for a streaming algorithm [22], allowing for continuous refinement of the graph weights, without increasing the size of the graph. The problem is that calculating the effective resistance between sets requires solving the Schur complement with respect to each set, which is computationally expensive; see Section A.1.

Remark 6.9. We note that the use of α -cover and region-wise scaling is not restricted to the region-based ER proposed in this paper. It can also be used for computing the standard ER.

7 Experiments

In this section, we demonstrate the region-based effective resistance (region-based ER) in the large graph limit and show that it converges to a meaningful limit. We divide the section into three sets of experiments. In Section 7.1, we replicate some of the experiments conducted in Von Luxburg et al. [13] and show that the region-based ER does not suffer from the trivial limit issue that standard ER suffer from. In Section 7.2 we take this a step further and demonstrate the convergence of region-based ER to a meaningful limit. Finally, in Section 7.3, we demonstrate a computationally efficient way to extend the calculations to large graphs in a controlled manner.

We note that to calculate the region-based ER, we utilize the Schur complement of the graph Laplacian with respect to these sets; see Appendix A.1 for more details.

Setting: Throughout this section, we consider standard ER and region-based ER on data sets $X_n \sim \mu^n(M)$, sampled from a distribution over a metric space (M, d) . For the standard ER we consider a resistor graph as described in Section 2. For the region-based ER we use a metric graph as defined in Definition 4.1. The standard ER between two nodes x_i, x_j in the graph is denoted $R_{ij} := R(x_i, x_j)$. For the region-based ER, we introduce the notation $R_{ij}^s := R_n(X_i, X_j)$. We use a radial kernel to determine the sets X_j, X_i associated with x_i, x_j . Namely $X_i = \{x \in X_n : \mathbb{1}(d(x, x_i) \leq r)\}$ and similarly for X_j . Here r_s is the source radius (which varies for each experiment).

7.1 Region-based ER does not converge to the Von-Luxburg limit

In this section, we replicate some of the experiments conducted in Von Luxburg et al. [13]. For the experiments, we calculate both the standard ER and the region-based ER proposed in this paper. We show that where the standard definition of ER converges to a trivial limit as shown by Von Luxburg et al. [13], the region-based ER does not.

We are interested in the convergence of the region-based ER compared to the standard ER as the number of samples used to construct the graph increases. We construct the graph on a sample X_n . Let $\eta_{ij} := 1/D_i + 1/D_j$ be the Von-Luxburg limit for the standard ER; similarly, let $\eta_{ij}^s := 1/D_i^s + 1/D_j^s$ be the Von-Luxburg limit for the region-based ER. Here D_i, D_j are the degrees of nodes i, j , respectively. Similarly, D_i^s, D_j^s are the degrees associated with the sets X_i, X_j , see Appendix E.1 and Lemma E.2 for more details. We then consider the max and mean of the relative deviation from the Von-Luxburg limit, namely:

$$\max_{ij} |R_{ij} - \eta_{ij}|/R_{ij} \quad \text{and} \quad \hat{\mathbb{E}}[|R_{ij} - \eta_{ij}|/R_{ij}]. \quad (7.1)$$

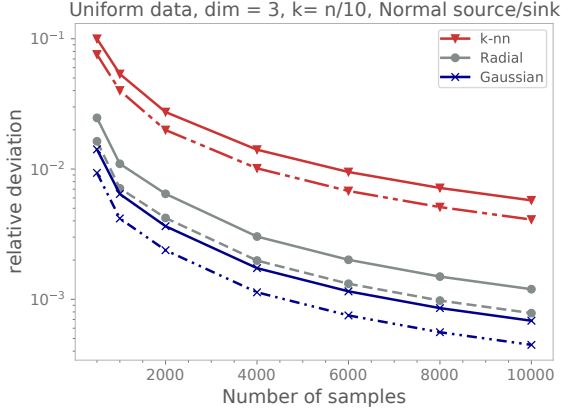
and

$$\max_{ij} |R_{ij}^s - \eta_{ij}^s|/R_{ij}^s \quad \text{and} \quad \hat{\mathbb{E}}[|R_{ij}^s - \eta_{ij}^s|/R_{ij}^s]. \quad (7.2)$$

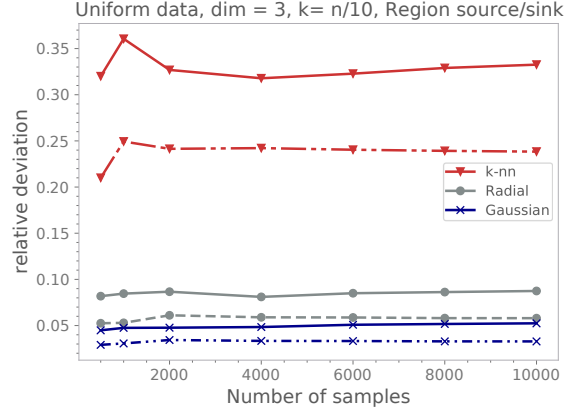
We consider the convergence of the relative deviation from the Von-Luxburg limit on two data sets that are similar to those studied in [13]. These are:

- ◇ Uniform 3-dim domain
- ◇ USPS data-set of handwritten digits (roughly 9200 samples in 256 dimensions)

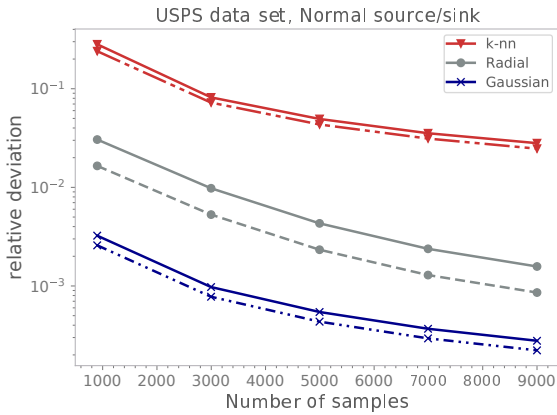
On each data set, we build a graph using the kernels outlined in section 3 and also include the nearest neighbor kernel, $\Gamma(x, y) = \mathbb{1}(y \in \mathcal{N}_\kappa(x)) \vee (x \in \mathcal{N}_\kappa(y))$ to better replicate the corresponding experiments in Von Luxburg et al. [13]. Similarly to these experiments, we also select the radius of the radial kernel and the bandwidth of the Gaussian kernel to be the maximal k-nn distance in the data. Note that for the USPS data set, we let $k = 100$, and for the uniform data set, we let $k = n/100$ where n is the number of samples. We let the source radius be the maximal 20-nn distance in the data.



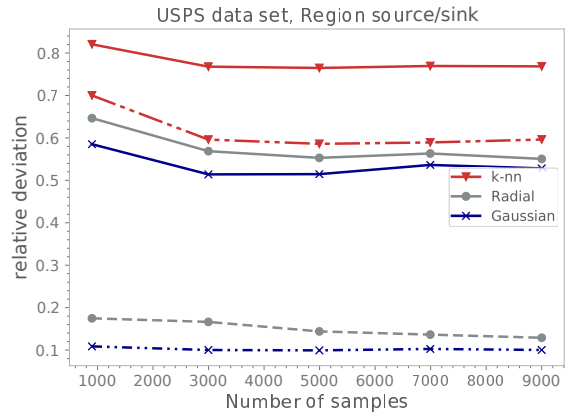
(a) Uniform domain/Standard ER



(b) Uniform domain/Region-based ER



(c) USPS data set/Standard ER



(d) USPS data set/Region-based ER

Figure 3: This figure demonstrates that standard ER converges to the Von-Luxburg limit, while region-based ER does not (which is a good thing). Here solid lines show maximal relative deviations, and dashed lines show mean relative deviations. The x-axis shows the number of samples used to construct the graph. The y-axis is the relative deviation of the effective resistance from the Von-Luxburg limit.

Uniform domain The results for the uniform domain are shown in Figure 3a-3b. The figure shows the max and mean relative deviation from the Von-Luxburg limit for the standard ER (Figure 3a) and the region-based ER (Figure 3b). We see that the standard ER converges quickly to the Von-Luxburg limit, which corresponds to the results in Von Luxburg et al. [13]. Meanwhile, we see that for the region-based ER, convergence to the Von-Luxburg limit does not occur, which confirms our theoretical results.

USPS data set A similar set of experiments is shown for the USPS data set in Figure 3c-3d. We observe the same behavior as for the uniform domain. The standard ER converges quickly to the Von-Luxburg limit, while the region-based ER does not converge to this limit. Again, this confirms our theoretical findings with respect to the region-based ER.

7.2 Meaningful limit

In the previous section, we saw that the region-based ER does not converge to the Von-Luxburg limit as was the case for the standard ER. However, it remains to be shown that the effective resistance under this new definition converges towards a meaningful limit. In this section, we take a closer look at this by considering the following two experiments

- ◇ Convergence to a meaningful limit on a half-moon of increasing density
- ◇ Meaningful ordering of points on a Swiss roll.

Half-moon experiment We consider a data distribution that consists of a background $[0, 1]^2$ with low density (10000 samples) and a half-moon with increasing density (samples in the interval $[100, \dots, 16000]$). This point cloud is illustrated in Figure 4a.

The purpose of this experiment is to demonstrate that the region-based ER converges to the "geodesic distance" along the half-moon (see the grey dotted line in Figure 4a), as the number of samples on the half-moon increases. This is a meaningful limit since the ER-based distance should consider all paths, and as the density of the half-moon becomes increasingly dominant, the distance should converge to the distance of paths along this curve.

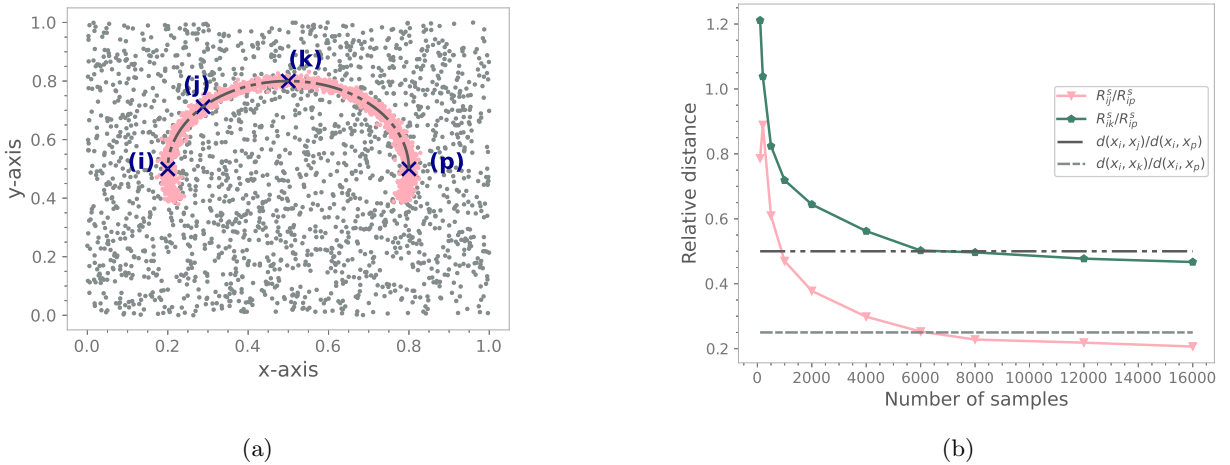


Figure 4: The region-based ER between points on the half-moon converges to the distance along the half-moon. (This is what we want to see). (a) High-density half-moon (pink) over low-density background (grey). The points we consider are labeled i, j, k , and p . (b) Grey dotted lines shows Γ_{ijp} and Γ_{ikp} (See Eq. (7.3)). Pink line shows R_{ij}^s/R_{ip}^s and Green line shows R_{ik}^s/R_{ip}^s .

The half-moon we consider is sampled from a circle segment with radius $t = 0.3$ and angle $\theta \in [-20, 200]^\circ$ with a Gaussian distribution $\mathcal{N}((t, \theta), 0.01)$ for each θ . Along the half-moon, we consider four points x_i, x_j, x_k , and x_p ; placed respectively at $\theta_i = 0^\circ$, $\theta_j = 45^\circ$, $\theta_k = 90^\circ$, and $\theta_p = 180^\circ$. We construct a graph on the point cloud using a radial kernel with radius $r = 0.08$. For the source and sink regions, we use a source radius $r_s = 0.05$ centered on each source-sink point, respectively.

Let $d(\cdot, \cdot)$ denote the distance along the half-moon arch as illustrated in Figure 4a by the grey dotted line. In order to compare the region-based ER distance with $d(\cdot, \cdot)$ we need to consider these distances relative to some reference distance. Because of this, we introduce the distance between points i and p as the reference. We then have

$$\Gamma_{ijp} := d(x_i, x_j)/d(x_i, x_p) = 0.25 \quad \text{and} \quad \Gamma_{ikp} := d(x_i, x_k)/d(x_i, x_p) = 0.5 \quad (7.3)$$

Figure 4b shows the region-based ER ratios R_{ij}^s/R_{ip}^s and R_{ik}^s/R_{ip}^s as the number of points sampled from the half moon increases. The ratios R_{ij}^s/R_{ip}^s and R_{ik}^s/R_{ip}^s converges towards Γ_{ijp} and Γ_{ikp} respectively. This is expected because, as the density on the half-moon increases, the effective resistance, which considers all possible paths, should be increasingly dominated by the paths along the half-moon.

Remark 7.1. We note that had the region-based ER converged to the Von-Luxburg limit, we would not have observed the convergence in Figure 4b. This is because the Von-Luxburg limit only depends on the degrees of the respective sets, which for the half-moon would be the same for all points i, j, k, p . Therefore, one would expect R_{ij}^s/R_{ip}^s and R_{ik}^s/R_{ip}^s to converge to 1 if this was the case.

Swiss roll experiment We consider a data distribution shaped as a Swiss roll and compare the relative distance between five points along the Swiss roll surface as indicated in Figure 5a. We consider the source radius $r_s = 0.1$ centered at the point and use a radial kernel with radius $r = 0.2$ to construct the graph.

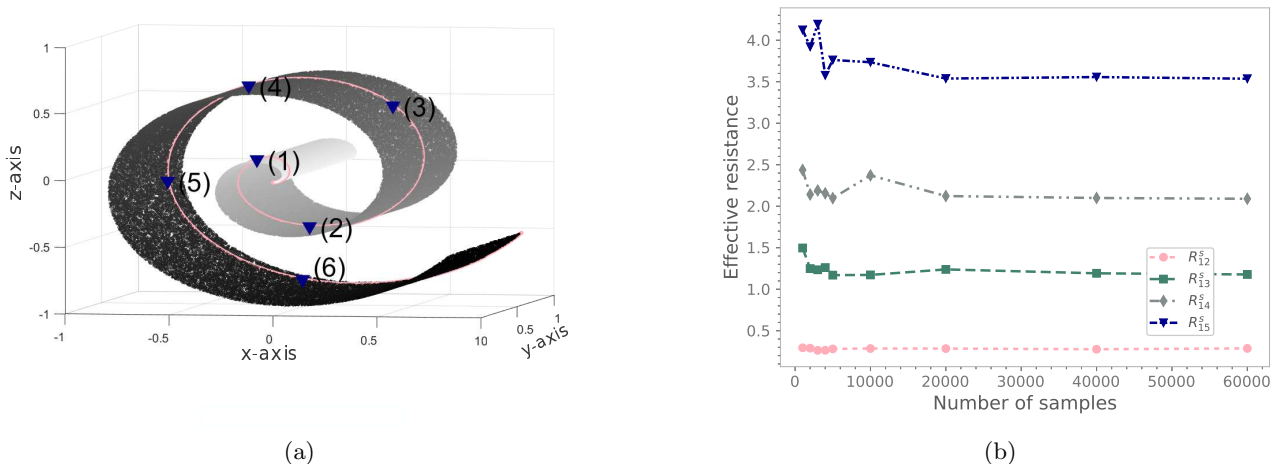


Figure 5: The ordering of the lines in (b) is meaningful (which is a good thing). Experiment demonstrating that the region-based ER distance gives a meaningful ordering of the distance between points and maintains this as the number of samples used to construct the graph increases. (a) Data distribution. Blue triangles indicate the location of the points $1, \dots, 6$. (b) The y-axis shows the region-based ER scaled by a factor of 10^{-5} . The x-axis shows the number of samples used to construct the graph. The pink line corresponds to the region-based ER R_{12}^s between 1, 2. Similarly, for R_{13}^s (green), R_{14}^s (gray), and R_{15}^s (blue).

The region-based ER R_{1i}^s between point 1 and respectively points $i \in [2, 3, 4, 5]$ is shown in Figure 5b. Using R_{1i}^s as a measure of distance between the points, we see that region-based ER gives a natural ordering of the distance from 1 to the other points, which is maintained as the number of samples increases. Namely, that $R_{12}^s < \dots < R_{15}^s$.

Remark 7.2. We note that had the region-based ER converged to the Von-Luxburg limit, this ordering would not have been maintained for the same reason as discussed in the half-moon experiment; See remark 7.1.

7.3 Example on the benefit of using an α -cover graph

We include a simple experiment to demonstrate the use of an α -cover and region-wise scaling, which was introduced in Section 6.1. We consider data sampled from a non-uniform density $\mu([0, 1])$ consisting of two regions of high density separated by a region of low density (See Figure 6). We consider five points $\mathcal{J} = \{1, \dots, 5\}$ marked by blue triangles in Figure 6 and calculate the region-based ER R_{1j}^s between 1 and points $j \in \mathcal{J} \setminus \{1\}$. In the experiment, the source radius is $r_s = 0.1$, and we use a radial kernel with radius $r = 0.1$.

We calculate the region-based ER using two different graphs;

- (A) Graph built on an α -cover with $\alpha = 2/3 \times 3^{-6}$ (1122 centers) and with region-wise scaling
- (B) Graph built with samples directly from $\mu([0, 1])$ and with point-wise scaling.

We note that in order to construct the α -cover, we use the cover-tree algorithm [20, 21].

In the experiment, the region-based ER R_{1j}^s between point 1 and points $j \in [2, 3, 4, 5]$ are calculated for both the α -cover graph with p_i scaling (A) and the density graph (B). Figure 7 shows that the region-based ER on the graph (A) converges to the same limit as the region-based ER on graph (B) when increasing the number of samples used to estimate the local probabilities p_i .

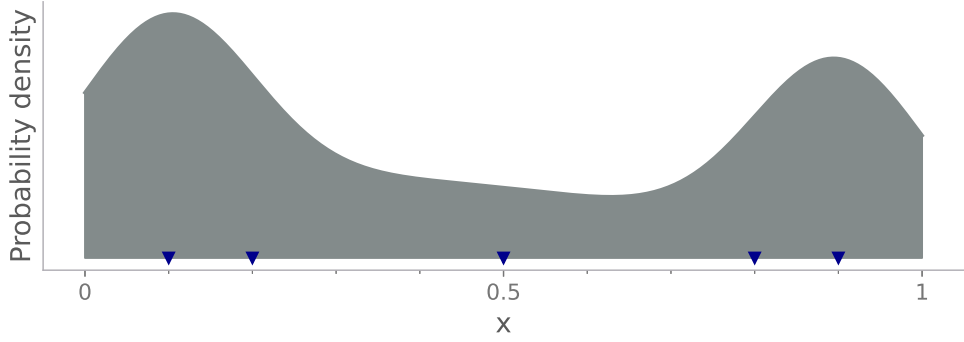
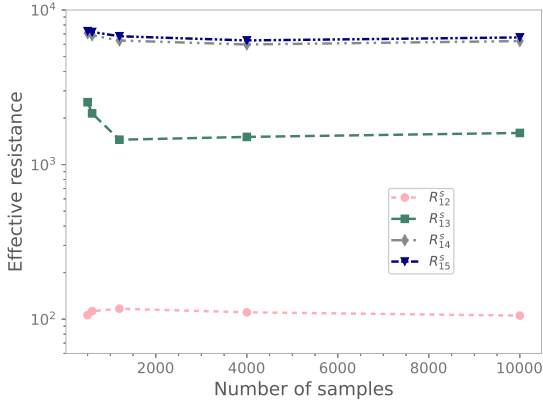
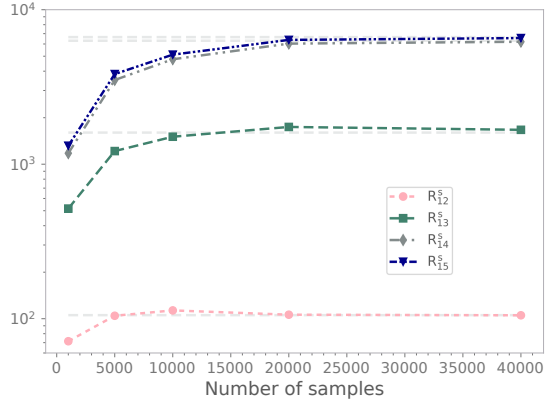


Figure 6: Non-uniform data distribution $\mu([0, 1])$. The y-axis shows the density of the data distribution $\mu([0, 1])$. The x-axis shows the support. The points we consider are marked by the blue triangles labeled (1), \dots , (5).

This is what we wanted to show because it means that region-based ER can be calculated in two ways, either using a graph constructed on an α -cover with appropriate scaling or by using a graph constructed directly on samples from $\mu([0, 1])$. The benefit of constructing the graph on the α -cover is that the graph size will be independent of the number of samples. At the same time, accuracy can still be increased by improving the estimates of the local probabilities p_i . This has the desirable property that it satisfies the condition of a streaming algorithm; See Section 6 for more details.



(a) Graph built on samples from density



(b) Graph built on α -cover with region-wise scaling

Figure 7: Demonstration of region-based ER on α -cover. We see that the ER in (b) converges to the asymptotics of the ER in (a) (weak gray lines). (This is a good thing). The dotted lines corresponds to region-based ER R_{1j}^s between point 1 and points $j \in [2, 3, 4, 5]$ respectively. The pink line corresponds to R_{12}^s , the green line to R_{13}^s , the grey line to R_{14}^s and the blue line to R_{15}^s . The y-axis shows the region-based ER, while the x-axis is different for each sub-figure. (a) x-axis shows the number of samples used to construct the graph. (b) x-axis shows the number of samples used to estimate the local probabilities p_i for scaling of the α -cover graph.

Furthermore, using an α -cover graph with region-wise scaling, a smaller graph can be used to calculate the region-based ER, provided sufficient samples are used to estimate the local probabilities p_i . Since estimating these local probabilities is cheap, time is saved. Table 1 illustrates this; the table has to be seen in relation to the convergence results in Figure 7.

Remark 7.3. *An additional note is that also for this experiment, using the region-based ER as a measure of distance gives a meaningful ordering, namely, $R_{12}^s < R_{13}^s < R_{14}^s < R_{15}^s$. Moreover, as more samples*

Table 1: Example of the time saved by calculating ER on an α -cover graph (graph A) instead of a graph constructed directly on the samples from the distribution (graph B). The first column shows the graphs used to calculate the ER; These are Graphs (A) and (B), described earlier. The second column is the number of samples used (The number in parenthesis is the size of the α -cover). The last column is the time to calculate the region-based ER using the Schur complement on the two graph types (The time in parenthesis is the time to estimate the local probabilities p_i for the α -cover).

Graph type	Number of samples	Time (s)
Graph (A)	21122 (1122)	0.04s + (0.07s)
Graph (B)	4000	4.6s

are used to estimate the local probabilities, the distance between the samples increases. Due to the shape of the density, it makes sense that the distance between points should be larger when the density is taken into account. Especially points separated by the region of low density, which is also what we observe.

Acknowledgments

AC was partially funded by NSF DMS 1819222 and 2012266, and a gift from Intel research. YF is funded by the NIH grant NINDS (PHS) U19NS107466 Reverse Engineering the Brain Stem Circuits that Govern Exploratory Behavior. RB is funded by NSF under CNS 1804829. AO is funded by Simula Research Laboratory.

References

- [1] Daniel A Spielman and Nikhil Srivastava. Graph sparsification by effective resistances. *SIAM Journal on Computing*, 40(6):1913–1926, 2011.
- [2] Mark Herbster and Massimiliano Pontil. Prediction on a graph with a perceptron. *Advances in neural information processing systems*, 19, 2006.
- [3] Teng Zhang and Changjiang Bu. Detecting community structure in complex networks via resistance distance. *Physica A: Statistical Mechanics and its Applications*, 526:120782, 2019.
- [4] Jihun Ham, Daniel D Lee, Sebastian Mika, and Bernhard Schölkopf. A kernel view of the dimensionality reduction of manifolds. In *Proceedings of the twenty-first international conference on Machine learning*, page 47, 2004.
- [5] Stefan Forcey and Drew Scalzo. Phylogenetic networks as circuits with resistance distance. *Frontiers in Genetics*, 11:1177, 2020.
- [6] Sotharith Tauch, William Liu, and Russel Pears. Measuring cascade effects in interdependent networks by using effective graph resistance. In *2015 IEEE Conference on Computer Communications Workshops (INFOCOM WKSHPS)*, pages 683–688, 2015.
- [7] Yakup Koç, Martijn Warnier, Piet Van Mieghem, Robert E. Kooij, and Frances M.T. Brazier. The impact of the topology on cascading failures in a power grid model. *Physica A: Statistical Mechanics and its Applications*, 402:169–179, 2014.
- [8] Xiangrong Wang, Yakup Koç, Robert E. Kooij, and Piet Van Mieghem. A network approach for power grid robustness against cascading failures. In *2015 7th International Workshop on Reliable Networks Design and Modeling (RNDM)*, pages 208–214, 2015.

- [9] Guido Cavraro and Vassilis Kekatos. Graph algorithms for topology identification using power grid probing. *IEEE Control Systems Letters*, 2(4):689–694, 2018.
- [10] László Lovász. Random walks on graphs. *Combinatorics, Paul erdos is eighty*, 2(1-46):4, 1993.
- [11] Stephen P Boyd, Arpita Ghosh, Balaji Prabhakar, and Devavrat Shah. Mixing times for random walks on geometric random graphs. In *ALLENEX/ANALCO*, pages 240–249, 2005.
- [12] Chen Avin and Gunes Ercal. On the cover time and mixing time of random geometric graphs. *Theoretical Computer Science*, 380(1-2):2–22, 2007.
- [13] Ulrike Luxburg, Agnes Radl, and Matthias Hein. Getting lost in space: Large sample analysis of the resistance distance. In *Advances in Neural Information Processing Systems*, volume 23. Curran Associates, Inc., 2010.
- [14] Ulrike Von Luxburg, Agnes Radl, and Matthias Hein. Hitting and commute times in large random neighborhood graphs. *The Journal of Machine Learning Research*, 15(1):1751–1798, 2014.
- [15] Yue Song, David J Hill, and Tao Liu. On extension of effective resistance with application to graph laplacian definiteness and power network stability. *IEEE Transactions on Circuits and Systems I: Regular Papers*, 66(11):4415–4428, 2019.
- [16] Douglas J Klein and Milan Randić. Resistance distance. *Journal of mathematical chemistry*, 12(1):81–95, 1993.
- [17] Palle ET Jorgensen and PJ Pearse Erin. Operator theory and analysis of infinite networks. *arXiv preprint arXiv:0806.3881*, 3, 2008.
- [18] Arpita Ghosh, Stephen Boyd, and Amin Saberi. Minimizing effective resistance of a graph. *SIAM Review*, 50(1):37–66, 2008.
- [19] Iqra Altaf Gillani and Amitabha Bagchi. A queueing network-based distributed laplacian solver for directed graphs. *Information Processing Letters*, 166:106040, 2021.
- [20] Alina Beygelzimer, Sham Kakade, and John Langford. Cover trees for nearest neighbor. In *Proceedings of the 23rd international conference on Machine learning*, pages 97–104, 2006.
- [21] Andreas Oslandsbotn, vZeljko Kereta, Valeriya Naumova, Yoav Freund, and Alexander Cloninger. Streamrak a streaming multi-resolution adaptive kernel algorithm. *Applied Mathematics and Computation*, 426:127112, 2022.
- [22] S. Muthukrishnan. Data streams: Algorithms and applications. *Foundations and Trends® in Theoretical Computer Science*, 1(2):117–236, 2005.
- [23] Ittai Abraham, Yair Bartal, and Ofer Neimany. Advances in metric embedding theory. In *Proceedings of the thirty-eighth annual ACM symposium on Theory of computing*, pages 271–286, 2006.

A Definitions

Definition A.1 (The doubling dimension). *(Adapted from [23])*

Let (M, d) be a metric space. The **doubling constant** of M is the minimal κ required to cover a ball $B_r(x)$ by κ balls of radius $r/2$, for all $x \in M$ and for all $r > 0$. The **doubling dimension** of X is defined as $ddim(M) = \log_2(\kappa)$.

A.1 Schur complement formulation of effective resistance between sets

[15] offered an explicit expression for the effective resistance between sets X_a, X_b in terms of the Schur complement. We restate this expression here, as we will use it when calculating the effective resistance for our experiments. Let L/L_{cc} be the Schur complement, Definition A.2, of the Laplacian L with respect to the block L_{cc} , where L_{cc} is the block corresponding to nodes in the set $X_c = X \setminus (X_a \cup X_b)$. The effective resistance between the sets X_a, X_b can then be defined as

$$R^s(X_a, X_b) = (e_{X_a}^\top (L/L_{cc}) e_{X_a})^{-1} \quad (\text{A.1})$$

where e_{X_a} is the vector with all ones for $i \in X_a$ and zero otherwise.

Definition A.2 (Schur complement). *Consider the block partition of the matrix $M = \begin{bmatrix} A & B \\ C & D \end{bmatrix}$, where $A \in \mathbb{R}^{n \times n}$, $B \in \mathbb{R}^{n \times m}$, $C \in \mathbb{R}^{m \times n}$ and $D \in \mathbb{R}^{m \times m}$. Provided D is non-singular, we define the Schur complement of M as $M/D = A - BD^{-1}C$.*

B Proof of Proposition 3.6

B.1 Properties of Contractions

In this section, we develop several tools that we will use throughout our entire proofs section. Let Z denote a space. We will be interested in functions, $v : Z \rightarrow \mathbb{R}$, as well as operators $A : v \mapsto (Av : Z \rightarrow \mathbb{R})$ that take functions to functions. For our purposes, Z will often be M , the underlying metric space, but will sometimes also be a finite sample from M .

We begin by defining the ℓ_∞ -norm, which will play a key role in our analysis.

Definition B.1. *Let $v : Z \rightarrow \mathbb{R}$ be a map. Then $\|v\|_\infty$ denotes the ℓ_∞ norm of v , and is defined as $\|v\|_\infty = \sup_{z \in Z} |v(z)|$.*

We can also define the ℓ_∞ -norm of an operator.

Definition B.2. *Let A be an operator, meaning it maps functions ($Z \rightarrow \mathbb{R}$) to other functions. Then*

$$\|A\|_\infty = \sup_{\|v\|_\infty > 0, v: Z \rightarrow \mathbb{R}} \frac{\|Av\|_\infty}{\|v\|_\infty}.$$

We will be especially interested in *contractions*, which are operators with infinity norm strictly less than 1. We are also interested in contractions combined with translations. We call such operators nice.

Definition B.3. *An operator, T , is **nice**, if there exists a contraction A and a map b such that $Tv = Av + b$.*

We are now prepared for our first useful result:

Lemma B.4. *Let T be a **nice** operator. Then there is a unique map $v : Z \rightarrow \mathbb{R}$ such that $Tv(z) = v(z)$ for all $z \in Z$.*

Proof. Let $Tv = Av + b$. Define $u_0 = b$ and $u_i = Tu_{i-1}$ for $i \geq 1$. Let $\|A\|_\infty = \rho$ where $0 \leq \rho < 1$ because T is nice. Observe that for $i \geq 1$,

$$\begin{aligned} \|u_{i+1} - u_i\|_\infty &= \|(Au_i(x) + b) - (Au_{i-1} + b)\|_\infty \\ &= \sup_{x \in M} \|A(u_i - u_{i-1})\|_\infty \\ &\leq \rho \|u_i - u_{i-1}\|_\infty. \end{aligned}$$

It follows that u_0, u_1, \dots is a Cauchy sequence under the ℓ_∞ metric. Since the set of all functions on the reals is closed, it follows that u_0, u_1, \dots , converges to some u , which must satisfy $Tu = u$.

To show uniqueness, we can simply bound the infinity distance between any two fixed points to see that this distance is at most ρ times itself. Since $\rho < 1$, it follows that the two fixed points must be the same function u . \square

We prove one addition lemma about nice operators.

Lemma B.5. *Let T be a nice operator with $Tv = Av + b$ where $\|A\|_\infty = \rho$. Suppose that function v satisfies $\|v - Tv\|_\infty < \epsilon$. If u denotes the unique fixed point of T , then*

$$\|u - v\|_\infty < \frac{\epsilon}{1 - \rho}.$$

Proof. By using the same argument as the previous lemma, we see that the sequence v, Tv, T^2v, \dots must converge to u . Since $\|v - Tv\|_\infty < \epsilon$, it follows that $\|T^i v - T^{i+1} v\| < \rho^i \epsilon$. Summing the infinite geometric sequence gives us the desired result. \square

B.2 Proving the existence of the energy-minimizing voltage (the limit object): Proposition 3.6

We begin by defining an operator that characterizes our desired limit object, v^* , (defined in Definition 3.1). In Lemma B.7 - B.9, we prove the existence and uniqueness of v^* . In Lemma B.10, we then prove that v^* is the energy-minimizing voltage from Definition 3.1.

Definition B.6. *Let k be a kernel and \hat{k} be the normalized version (Definition 3.2). Then A_* is the operator defined as follows. If $v : M \rightarrow \mathbb{R}$ is a measurable function, then A_*v is the function $M \rightarrow \mathbb{R}$ defined by*

$$(A_*v)(x) = \int_M v^*(y) \hat{k}(x, y) \mathbb{1}(y \in M \setminus (M_g \cup M_s)) d\mu(y).$$

We also let $b_* : M \rightarrow \mathbb{R}$ denote the fixed function defined as

$$b_*(x) = \int_M \hat{k}(x, y) \mathbb{1}(y \in M_s) d\mu(y).$$

Together, we let T_* be the operator

$$T_*v = A_*v + b_*.$$

Our main idea will be to show the following two statements holds:

1. There exists $m > 0$ such that T_*^m is contractive (Definition B.3).
2. v^* is a fixed point of T_* .

Together with Lemma B.4, this will prove the existence and uniqueness of v^* . We start by proving the first claim, which relies on the following technical Lemma that characterizes iterative powers of A_* .

Lemma B.7. *Let $v : M \rightarrow \mathbb{R}$ be a measurable map and $x \in M$ be a point. Then for all $i \geq 1$,*

$$|(A_*^i v)(x)| \leq \int_M |v(y)| \hat{k}^{(i)}(x, y) \mathbb{1}(y \in M \setminus (M_g \cup M_s)).$$

Proof. We proceed by induction on i . In the base case, $i = 1$, and we have

$$\begin{aligned} |(A_*v)(x)| &= \left| \int_M v(y) \hat{k}(x, y) \mathbb{1}(y \in M \setminus (M_g \cup M_s)) d\mu(y) \right| \\ &\leq \int_M |v(y)| \hat{k}(x, y) \mathbb{1}(y \in M \setminus (M_g \cup M_s)) d\mu(y) \\ &\leq \int_M |v(y)| \hat{k}(x, y) d\mu(y). \end{aligned}$$

For the inductive step, let $i > 1$ and assume that the claim holds for $i - 1$. Then

$$\begin{aligned} |(A_*^i v)(x)| &= |(A_*(A_*^{(i-1)} v))(x)| \\ &= \left| \int_M (A_*^{(i-1)} v)(y) \hat{k}(x, y) \mathbb{1}(y \in M \setminus (M_g \cup M_s)) d\mu(y) \right| \\ &\leq \int_M |(A_*^{(i-1)} v)(y)| \hat{k}(x, y) \mathbb{1}(y \in M \setminus (M_g \cup M_s)) d\mu(y) \\ &\leq \int_M |(A_*^{(i-1)} v)(y)| \hat{k}(x, y) d\mu(y) \\ &\leq \int_M \left(\int_M |v(z)| \hat{k}^{(i-1)}(y, z) \mathbb{1}(z \in M \setminus (M_g \cup M_s)) d\mu(z) \right) \hat{k}(x, y) d\mu(y) \\ &= \int_M \left(\int_M \hat{k}(x, y) \hat{k}^{(i-1)}(y, z) d\mu(y) \right) |v(z)| \mathbb{1}(z \in M \setminus (M_g \cup M_s)) d\mu(z) \\ &= \int_M |v(z)| \hat{k}^{(i)}(x, z) \mathbb{1}(z \in M \setminus (M_g \cup M_s)) d\mu(z), \end{aligned}$$

as desired. Here the inequalities hold by

1. Moving the absolute value into the expectation.
2. bounding the indicator function by 1.
3. Applying the inductive hypothesis.
4. Applying Fubini's theorem to switch the order.
5. Applying convolution (Definition 3.4).

□

We now show that there exists a power of A_* that is a contraction.

Lemma B.8. *Let α be as in the statement of Proposition 3.6. Then for all maps $v : M \rightarrow \mathbb{R}$,*

$$\sup_{x \in M} |(A_*^m v)(x)| \leq (1 - \alpha) \sup_{x \in M} |v(x)|.$$

Proof. Fix $x \in M$. Then by applying Lemma B.7,

$$\begin{aligned} |(A_*^m v)(x)| &\leq \int_M |v(y)| \hat{k}^{(m)}(x, y) \mathbb{1}(y \in M \setminus (M_g \cup M_s)) d\mu(y) \\ &\leq \sup_{x \in M} |v(x)| \int_M \hat{k}^{(m)}(x, y) \mathbb{1}(y \in M \setminus (M_g \cup M_s)) d\mu(y). \end{aligned}$$

Because \hat{k} is normalized, $\hat{k}^{(m)}$ is as well, meaning that $\int_M \hat{k}^{(m)}(x, y) d\mu(y) = 1$. However, we also have by assumption (Proposition 3.6) that $M = C_\alpha^m(M_g \cup M_s)$, which implies that

$$\int_M \hat{k}^{(m)}(x, y) \mathbb{1}(y \in M_g \cup M_s) d\mu(y) \geq \alpha.$$

Substituting this, it follows that

$$\begin{aligned} |(A_*^m v)(x)| &\leq \sup_{x \in M} |v(x)| \int_M \hat{k}^{(m)}(x, y) \mathbb{1}(y \in M \setminus (M_g \cup M_s)) d\mu(y). \\ &\leq (1 - \alpha) \sup_{x \in M} |v(x)| \end{aligned}$$

□

We are now prepared to show that there exists a unique fixed point of T_* .

Lemma B.9. *There exists a unique function $v^* : M \rightarrow [0, 1]$ such that $T_* v^* = v^*$.*

Proof. Let m be as in Lemma B.8. Observe that the operator $T_*^m v$ can be written as

$$T_*^m : v \mapsto A_*^m v + b_*(x) + (A_* b_*)(x) + \cdots + (A_*^{m-1} b_*)(x).$$

By Lemma B.8, A_*^m is a contraction and therefore T_*^m is a nice (Definition B.3) operator. It follows by Lemma B.4 that T_*^m has a unique fixed point which we denote as v^* .

Any fixed point of T_* is a fixed point of T_*^m , and therefore it suffices to show that v^* is a fixed point of T_* – uniqueness will follow from the uniqueness of v^* w.r.t. T_*^m . To do so, observe that

$$T_*^m(T_* v^*) = T_*^m(T_* v^*) = T_*(T_*^m v^*) = T_*(v^*).$$

Thus $T_* v^*$ is a fixed point of T_*^m , meaning that it must equal v^* by the uniqueness of v^* . Thus $T_* v^* = v^*$, as desired. □

We now show that v^* is the energy-minimizing voltage of the energy defined in Definition 3.1.

Lemma B.10. *Let $M_s, M_g \subset M$ be measurable disjoint subsets. Let V_{M_s, M_g} be the set of all measurable functions $v : M \rightarrow [0, 1]$ with $v(x) = 1$ for all $x \in M_s$ and $v(x) = 0$ for all $x \in M_g$. The minimizer of the energy $E(v)$ defined in Definition 3.1, is the function $v \in V_{M_s, M_g}$ that satisfies $v^* = T_* v^*$.*

Proof. To show that v^* is a minimizer of $E(v)$ from Definition 3.1, it is sufficient to show that the following two statements hold.

1. If $v^* = T_* v^*$ then $E(v^*) < E(u)$ for all $u \in V_{M_s, M_g}$, $u \neq v^*$
2. If $E(v^* + u) \geq E(v^*)$ for all $u \in V_{M_s, M_g}$ then $v^* = T_* v^*$

Let $\varepsilon > 0$ and $v \in V_{M_s, M_g}$. Consider $u = v^* + \varepsilon v \in V_{M_s, M_g}$ and the energy from Definition 3.1 evaluated at u namely

$$\begin{aligned} E(u) &= E(v^* + \varepsilon v) = \int_M \int_M \hat{k}(x, y) [(v^*(x) + \varepsilon v(x)) - (v^*(y) + \varepsilon v(y))]^2 d\mu(x) d\mu(y) \\ &= \int_M \int_M \hat{k}(x, y) (v^*(x) - v^*(y))^2 d\mu(x) d\mu(y) \\ &\quad - 2\varepsilon \int_M \int_M \hat{k}(x, y) (v^*(x) - v^*(y))(v(x) - v(y)) d\mu(x) d\mu(y) \\ &\quad + \varepsilon^2 \int_M \int_M \hat{k}(x, y) (v(x) - v(y))^2 d\mu(x) d\mu(y) \\ &= E(v^*) + \varepsilon^2 E(v) - 4\varepsilon E(v^*, v). \end{aligned}$$

Here $E(v^*, v) := \frac{1}{2} \int_M \int_M \hat{k}(x, y) (v^*(x) - v^*(y))(v(x) - v(y)) d\mu(x) d\mu(y)$. We then have

$$E(v^*) = E(v^* + \varepsilon v) - \varepsilon^2 E(v) + 4\varepsilon E(v^*, v) \tag{B.1}$$

For the first statement, if $v = T_*v^*$ it follows from Lemma B.11 that $E(v^*, v) = 0$. Consequently, with $\varepsilon = 1$,

$$E(v^*) = E(v^* + \varepsilon v) - E(v).$$

Since $E(v^* + \varepsilon v) > 0$ and $E(v) > 0$ it follows that $E(v^*) < E(v^* + \varepsilon v)$. Because u was arbitrary, the first statement holds.

For the second statement, if $E(v^* + \varepsilon v) \geq E(v^*)$ then from Eq. (B.1) we require $4\varepsilon E(v^*, v) - \varepsilon^2 E(v) \leq 0$. In other words, $\varepsilon E(v) \geq 4E(v^*, v)$ for any $\varepsilon > 0$. Since ε can be arbitrarily small, this means we need $E(v^*, v) = 0$. From Lemma B.11 it follows that if $E(v^*, v) = 0$ for all $v \in V_{M_s, M_g}$ then $v^* = Tv^*$. Consequently, the second statement holds. \square

Lemma B.11. Consider the bilinear energy $E(v^*, v) = \frac{1}{2} \int_M \int_M \hat{k}(x, y)(v^*(x) - v^*(y))(v(x) - v(y))d\mu(x)d\mu(y)$ defined in lemma B.10.

1. If $v^* = T_*v^*$ then $E(v^*, v) = 0$ for all $v \in V_{M_s, M_g}$
2. If $E(v^*, v) = 0$ for all $v \in V_{M_s, M_g}$ then $v^* = T_*v^*$

Proof. From Lemma B.12 it follows that

$$E(v^*, v) = \int_M v(x)[v^*(x) - (Tv^*)(x)]d\mu(x).$$

Consequently, if $v^* = T_*v^*$, then $E(v^*, v) = \int_M v(x)[v^*(x) - v^*(x)]d\mu(x) = 0$ for all $v \in V_{M_s, M_g}$. Now, consider the second statement. If $E(v^*, v) = 0$ for all $v \in V_{M_s, M_g}$ then we require $v^* - Tv^* = 0$. Consequently, $v^* = Tv^*$. \square

Lemma B.12. The bilinear energy form

$$E(v^*, v) = \frac{1}{2} \int_M \int_M \hat{k}(x, y)(v^*(x) - v^*(y))(v(x) - v(y))d\mu(x)d\mu(y)$$

can be written as

$$E(v^*, v) = \int_M v(x)[v^*(x) - (Tv^*)(x)]d\mu(x).$$

Proof. We have

$$\begin{aligned} E(v^*, v) &= \frac{1}{2} \int_M \int_M \hat{k}(x, y)v^*(x)v(x)d\mu(x)d\mu(y) + \frac{1}{2} \int_M \int_M \hat{k}(x, y)v^*(y)v(y)d\mu(x)d\mu(y) \\ &\quad - \frac{1}{2} \int_M \int_M \hat{k}(x, y)v^*(x)v(y)d\mu(x)d\mu(y) - \frac{1}{2} \int_M \int_M \hat{k}(x, y)v^*(y)v(x)d\mu(x)d\mu(y) \\ &= \underbrace{\int_M \int_M \hat{k}(x, y)v^*(x)v(x)d\mu(x)d\mu(y)}_{I_1} - \underbrace{\int_M \int_M \hat{k}(x, y)v^*(y)v(x)d\mu(x)d\mu(y)}_{I_2} \end{aligned}$$

For I_1 we have

$$\begin{aligned} \int_M \int_M \hat{k}(x, y)v^*(x)v(x)d\mu(x)d\mu(y) &= \int_M \left(\int_M \hat{k}(x, y)d\mu(y) \right) v^*(x)v(x)d\mu(x) \\ &= \int_M v^*(x)v(x)d\mu(x). \end{aligned}$$

In the last step, we used that $\int_M \hat{k}(x, y)d\mu(y) = 1$, since from Definition 3.2 we have $\hat{k}(x, y) = k(x, y) / \int_M k(x, z)d\mu(z)$. For I_2 we have

$$\begin{aligned} \int_M \int_M \hat{k}(x, y)v^*(y)v(x)d\mu(x)d\mu(y) &= \int_M v(x) \left(\int_M \hat{k}(x, y)v^*(y)d\mu(y) \right) d\mu(x) \\ &= \int_M v(x)(T_*v^*)(x)d\mu(x) \end{aligned}$$

It follows that

$$E(v^*, v) = \int_M [v^*(x)v(x) - v(x)(Tv^*)(x)]d\mu(x) = \int_M v(x)[v^*(x) - (Tv^*)(x)]d\mu(x)$$

□

C Proofs from Analysis Section

In this section, our goal will be to show that effective resistances computed over metric graphs that are sampled from M will converge towards the desired limit object. We begin with some technical results for approximating integrals with sums over finite samples from μ .

C.1 Bounding integrals of functions

We begin by stating Hoeffding's bound for a map $f : M \rightarrow [0, 1]$, $\int_M f(y)d\mu(y)$ can be approximated with the sum $\frac{1}{n} \sum_{i=1}^n f(x_i)$.

Lemma C.1 (Hoeffding). *Let $S_n \sim \mu^n$ be n i.i.d draws with $S_n = \{x_1, \dots, x_n\}$, and let $f : M \rightarrow [0, 1]$ be a map. Then,*

$$\Pr \left[\left| \int_M f(y)d\mu(y) - \frac{1}{n} \sum_{i=1}^n f(x_i) \right| > \epsilon \right] \leq 2 \exp(-2n\epsilon^2).$$

Next, we bound the quotient of two integrals.

Lemma C.2. *Let $S_n \sim \mu^n$ be n i.i.d draws with $S_n = \{x_1, \dots, x_n\}$, and let $f : M \rightarrow [0, 1]$ and $g : M \rightarrow [0, 1]$ be two maps. Suppose that $\int_M g(y)d\mu(y) \geq G$. Then*

$$\Pr \left[\left| \frac{\int_M f(y)d\mu(y)}{\int_M g(y)d\mu(y)} - \frac{\frac{1}{n} \sum_{i=1}^n f(x_i)}{\frac{1}{n} \sum_{i=1}^n g(x_i)} \right| > \epsilon \right] \leq 4 \exp(-8nG^2\epsilon^2).$$

Proof. It suffices to bound the probability that

$$\left| \int_M f(y)d\mu(y) - \frac{1}{n} \sum_{i=1}^n f(x_i) \right| < \frac{\epsilon}{4}$$

and

$$\left| \int_M g(y)d\mu(y) - \frac{1}{n} \sum_{i=1}^n g(x_i) \right| < \frac{G\epsilon}{4}$$

as these two equations imply the desired bound by straightforward algebra. The probability that both of these occur can be bounded by a union bound after applying Hoeffding's inequality twice. □

C.2 Showing that A_n^m is a contraction

We define the *finite* analogs of A_* and b_* (Definition B.6).

Definition C.3. *Let $S_n \sim \mu^n$ be a sample of n points, x_1, \dots, x_n . Let $v : S_n \rightarrow \mathbb{R}$ be a map. Then the operators A_n and the map b_n are defined as*

$$(A_n v)(x) = \frac{\sum_{i=1}^n k(x, x_i)v(x_i)\mathbb{1}(x_i \in M \setminus (M_0 \cup M_1))}{\sum_{i=1}^n k(x, x_i)},$$

and

$$b_n(x) = \frac{\sum_{i=1}^n k(x, x_i)\mathbb{1}(x_i \in M_1)}{\sum_{i=1}^n k(x, x_i)}.$$

Our goal in this section is to show that A_n^m is also a contraction, where m is as defined in the statement of Theorem 4.4.

We first define the parameter K as follows.

Definition C.4. Let K be the inverse of the minimal degree in M . That is, let

$$K = \max_{x \in M} \frac{1}{\int_M k(x, y) d\mu(y)}.$$

This is well defined because M is compact and because $\int_M k(x, y) d\mu(y)$ is both continuous and larger than 0 by assumption. Because k has range in $[0, 1]$, it follows that

$$\max_{x \in M} \hat{k}(x) \leq K \tag{C.1}$$

where \hat{k} is the normalized kernel defined in Definition 3.2.

We now prove a technical lemma that will assist us in understanding the structure of G_n , the metric graph built over a finite sample $S_n \sim \mu^n$.

Lemma C.5. Let $P \subseteq M$ be a measurable set, and let $i > 1$. Let $p > 0$ and suppose that for all $x \in M$,

$$\int_M \hat{k}^{(i)}(x, y) \mathbb{1}(y \in P) d\mu(y) \geq p.$$

Then there exists a measurable subset $Q \subseteq M$ such that the following two properties hold:

- For all $x \in M$, $\int_M \hat{k}^{(i-1)}(x, y) \mathbb{1}(y \in Q) d\mu(y) \geq \frac{p}{2K-p}$, with K as defined above.
- For all $x \in Q$, $\int \hat{k}(x, y) \mathbb{1}(y \in P) d\mu(y) \geq \frac{p}{2}$.

Proof. Observe that by the definition of convolution and Fubini's theorem,

$$\begin{aligned} \int_M \hat{k}^{(i)}(x, y) \mathbb{1}(y \in P) d\mu(y) &= \int_M (\hat{k}^{(i-1)} \circ \hat{k})(x, y) \mathbb{1}(y \in P) d\mu(y) \\ &= \int_M \left(\int_M \hat{k}^{(i-1)}(x, z) \hat{k}(z, y) d\mu(z) \right) \mathbb{1}(y \in P) d\mu(y) \\ &= \int_M \hat{k}^{(i-1)}(x, z) \left(\int_M \hat{k}(z, y) \mathbb{1}(y \in P) d\mu(y) \right) d\mu(z). \end{aligned}$$

Define $f(z) = \int_M \hat{k}(z, y) \mathbb{1}(y \in P) d\mu(y)$. Since $\hat{k} \leq K$, it follows that f has range $[0, K]$. We now define $Q = \{z : f(z) \geq \frac{p}{2}\}$, and claim that this suffices. By definition, the second property trivially holds. To see that the first property holds, let $q = \int_M \hat{k}^{(i-1)}(x, y) \mathbb{1}(y \in Q) d\mu(y)$. Then,

$$\begin{aligned} p &\leq \int_M \hat{k}^{(i)}(x, y) \mathbb{1}(y \in P) d\mu(y) \\ &= \int_M \hat{k}^{(i-1)}(x, z) \left(\int_M \hat{k}(z, y) \mathbb{1}(y \in P) d\mu(y) \right) d\mu(z) \\ &= \int_M \hat{k}^{(i-1)}(x, z) f(z) d\mu(z) \\ &= \int_Q \hat{k}^{(i-1)}(x, z) f(z) d\mu(z) + \int_{M \setminus Q} \hat{k}^{(i-1)}(x, z) f(z) d\mu(z) \\ &\leq Kq + \left(\frac{p}{2}\right) (1 - q). \end{aligned}$$

Rearranging this gives the desired inequality. □

Recall that m and α are defined in the statement of Theorem 4.4 such that $M = C_\alpha^m(M_1 \cup M_0)$. We have the following lemma which gives additional structure to M .

Lemma C.6. *There exists sets $P_0, P_1, P_2, \dots, P_m \subseteq M$ with $P_0 = M$ and $P_m = M_0 \cup M_1$ such that the following holds. There exists positive reals p_1, p_2, \dots, p_m such that for all $1 \leq i \leq m$, for all $x \in P_{i-1}$,*

$$\int_M \hat{k}(x, y) \mathbb{1}(y \in P_i) d\mu(y) \geq p_i.$$

Proof. The idea is simple: we apply Lemma C.5 m times starting with $P_m = M_0 \cup M_1$. To establish the base case, recall that $M = C_\alpha^m(M_1 \cup M_0)$, which implies

$$\int_M \hat{k}^{(m)}(x, y) \mathbb{1}(y \in P_m) d\mu(y) \geq \alpha$$

for $\alpha > 0$.

Define $q_m = \alpha$. We will now show how to recursively construct P_i , q_{i-1} and p_i from q_i . Suppose that for all $x \in M$,

$$\int_M \hat{k}^{(i)}(x, y) \mathbb{1}(y \in P_i) d\mu(y) \geq q_i. \quad (\text{C.2})$$

Then applying Lemma C.5, we let $P_{i-1} = Q$, $p_i = \frac{q_i}{2}$, and $q_{i-1} = \frac{q_i}{2k - q_i}$. It is easy to see by Lemma C.5 that doing so preserves Equation C.2 and that p_i satisfies the desired equation.

Finally, in the case that $i = 1$, we can simply let $p_1 = q_1$, as we no longer require Lemma C.5 since $\hat{k}^{(1)} = \hat{k}$. This completes the proof. \square

We are now prepared to show that A_n^m is indeed a contraction over S_n .

Lemma C.7. *There exists an absolute constant $p > 0$ independent of n and S_n such that the following holds.*

$$\lim_{n \rightarrow \infty} \Pr_{S_n \sim \mu^n} [\|A_n^m\|_\infty \leq 1 - p] = 1.$$

Proof. Fix P_0, \dots, P_m and p_0, p_1, \dots, p_m as in Lemma C.6. Let E denote the event that for all $1 \leq i \leq n$ and $1 \leq j \leq m$ such that $x_i \in P_{j-1}$,

$$\frac{\frac{1}{n} \sum_{t=1}^n k(x_i, x_t) \mathbb{1}(x_t \in P_j)}{\frac{1}{n} \sum_{t=1}^n k(x_i, x_t)} \geq \frac{p_j}{2}.$$

The key observation is that by applying Lemma C.2 to all mn pairs of points along with a union bound, there exists an absolute constant C for which $\Pr[E] \geq 1 - nm \exp(-nC)$. Thus for n sufficiently large, the probability of E converges to 1. This is a direct result of the fact that by Lemma C.6,

$$\int_M \hat{k}(x_i, y) \mathbb{1}(y \in P_j) d\mu(y) \geq p_j,$$

whenever $x_i \in P_{j-1}$. Note that although there is a technical independence issue as the function $x_t \rightarrow k(x_i, x_t)$ has a dependence on x_i which is in S_n , this can be resolved by observing that for any function f , for n sufficiently large, $\left| \frac{1}{n} \sum f(x_j) - \frac{1}{n-1} \sum_{j \neq i} f(x_j) \right|$ is small.

Finally, given that the event E occurs, we can bound $\|A_n^m\|_\infty$ as follows. For any $v : S_n \rightarrow \mathbb{R}$, we have from Definition C.3,

$$\begin{aligned} |A_n^v(x)| &\leq \sum_{t_1=1}^n \frac{k(x, x_{t_1})}{\sum_{i=1}^n k(x, x_i)} \sum_{t_2=1}^n \frac{k(x_{t_1}, x_{t_2})}{\sum_{i=1}^n k(x_{t_2}, x_i)} \cdots \sum_{t_m=1}^n \frac{k(x_{t_{m-1}}, x_{t_m})}{\sum_{i=1}^n k(x_{t_m}, x_i)} \mathbb{1}(x_{t_m} \in M \setminus (M_1 \cup M_0)) \\ &= 1 - \sum_{t_1=1}^n \frac{k(x, x_{t_1})}{\sum_{i=1}^n k(x, x_i)} \sum_{t_2=1}^n \frac{k(x_{t_1}, x_{t_2})}{\sum_{i=1}^n k(x_{t_2}, x_i)} \cdots \sum_{t_m=1}^n \frac{k(x_{t_{m-1}}, x_{t_m})}{\sum_{i=1}^n k(x_{t_m}, x_i)} \mathbb{1}(x_{t_m} \in M_1 \cup M_0) \\ &\leq 1 - \sum_{x_{t_1} \in P_1} \frac{k(x, x_{t_1})}{\sum_{i=1}^n k(x, x_i)} \sum_{x_{t_2} \in P_2} \frac{k(x_{t_1}, x_{t_2})}{\sum_{i=1}^n k(x_{t_2}, x_i)} \cdots \sum_{x_{t_m} \in P_m} \frac{k(x_{t_{m-1}}, x_{t_m})}{\sum_{i=1}^n k(x_{t_m}, x_i)} \mathbb{1}(x_{t_m} \in M_1 \cup M_0) \\ &\leq 1 - \frac{\prod_{i=1}^m p_i}{2^m}. \end{aligned}$$

Thus selecting $p = \frac{\prod_{i=1}^m p_i}{2^m}$ suffices, as desired. \square

As a quick remark, although the factor of contraction shown here is *extremely* close to 1, this analysis is just considering worst-case situations in which M has a very complicated structure. In most actual cases, the factor of contraction is far far smaller.

C.3 Finishing the proof

We are now prepared to compare v^* with v_n^* . The key idea is to restrict v^* to S_n and then compare it with $A_n^m v^*$. We begin with the following lemma.

Lemma C.8. *Let $u : M \rightarrow [0, 1]$ be a measurable function, $x \in M$ be a point, and $\epsilon > 0$ be a real number. Then there exists a constant C such that*

$$\Pr_{S \sim \mu^n} [|(A_* u + b_*)(x) - (A_n u + b_n)(x)| > \epsilon] < 4 \exp(-Cn\epsilon^2).$$

Proof. We will examine $|A_* u - A_n u|$ and $|b_* - b_n|$ separately and then apply the triangle inequality. Let $M' = M \setminus (M_1 \cup M_0)$. Then,

$$|(A_* u)(x) - (A_n u)(x)| = \left| \frac{\int_M k(x, y) u(y) d\mu(y)}{\int_M k(x, y) d\mu(y)} - \frac{\frac{1}{n} \sum_{x_i \in M'} k(x, x_i) u(x_i)}{\frac{1}{n} \sum_{x_i \in M'} k(x, x_i)} \right|.$$

However, by Lemma C.2, this quantity is at most ϵ with probability $2 \exp(-O(n\epsilon^2))$. We can apply a similar argument for $b_* - b_n$ which completes the proof. \square

Lemma C.9. *Restrict v^* and b_* (definition B.6) to S_n . Then $\|v^* - (A_n v^* + b_n)\|_\infty \rightarrow 0$ and $\|b_* - b_n\|_\infty \rightarrow 0$ in probability. Here again, the infinity norms are taken over S_n , not M .*

Proof. Simply apply Lemma C.8 for all $x = x_i$ and $u = v^*$ and then apply a union bound. While there are technically independence issues, this is solved by observing that x_i is independent of all other elements of S_n , and the averages taken over S_n ignoring x_i are barely different from those including x_i . \square

Lemma C.10. *Let $c_n = b_n + A_n b_n + A_n^2 b_n + \dots + A_n^{m-1} b_n$. Then $\|v^* - (A_n^m v^* + c_n)\|_\infty \rightarrow 0$ in probability.*

Proof. The key idea is that A_n is at most an averaging operator, and consequently $\|A_n\| \leq 1$. Intuitively, applying A_n to a map $v : S_n \rightarrow \mathbb{R}$ cannot increase $\max_{x \in S_n} |v(x)|$. Let $T_n v = A_n v + b_n$. This implies that for all u and v ,

$$\|u - v\|_\infty \geq \|T_n u - T_n v\|.$$

Applying this m times along with the triangle inequality, we see that

$$|v^* - T_n^m v^*| \leq (m - 1) |v^* - T_n v^*|.$$

However, since the latter goes to 0 in probability, it follows that the former does as well. All that remains to see is that $T_n^m v$ precisely equals $A_n^m v^* + c_n$, as desired. \square

We can finally prove Theorem 4.4.

Proof. By the previous Lemma, for any $\epsilon > 0$ and $\delta > 0$ there exists n such that with probability $1 - \delta$, $\|v^* - (A_n^m v^* + c_n)\|_\infty < \epsilon$. Since A_n^m is a contraction, it follows by Lemma B.5 that v^* has distance at most $\frac{\epsilon}{p}$ from v_n^* , the fixed point of $v \mapsto A_n^m v + c_n$. Since p is fixed, it follows that $|v_n^* - v^*|_\infty \rightarrow 0$. Finally, for an arbitrary point $x \in M$, simply applying Lemma C.2 one last time over the definition of $v_n^*(x)$ implies the desired result. \square

D Proof of Convergence using α -covers

Here, our goal is to prove Theorem 6.8. To do so, we impose an additional technical restriction on our kernel k .

Definition D.1. Let μ be a measure over metric space M , and let $k : M \times M \rightarrow [0, 1]$ be a kernel. Let $V \subset M \times M$ denote the set of all (x, y) for which k is continuous at (x, y) , and let $\mu \times \mu$ denote the product measure over $M \times M$. Then k is said to be μ -**continuous** if

$$(\mu \times \mu)((M \times M) \setminus V) = 0.$$

It is easy to verify that for most common measures over \mathbb{R}^d that the Gaussian and Radial kernels are μ -continuous.

We now assume that k is a μ -continuous kernel, and moreover that

Next, we define an analog to the quantities A_n and b_n with respect to our α -cover \mathcal{C} .

Definition D.2. Let $S \sim \mu^n$ be an i.i.d sample of data, and let $\mathcal{C} = \{c_1, \dots, c_m\}$ be an α -cover. Let $\gamma_{i,n}$ denote the fraction of points from S that lie in the cell corresponding to c_i . Let $v : \mathcal{C} \rightarrow \mathbb{R}$ be a map. Then the operators $A_{\mathcal{C},n}$ and the map $b_{\mathcal{C},n}$ are defined as

$$(A_{\mathcal{C},n}v)(x) = \frac{\sum_{i=1}^m k(x, c_i)v(c_i)\gamma_{i,n}\mathbb{1}(c_i \in M \setminus (M_0 \cup M_1))}{\sum_{i=1}^m \gamma_{i,n}k(x, c_i)},$$

and

$$b_{\mathcal{C},n}(x) = \frac{\sum_{i=1}^m \gamma_{i,n}k(x, c_i)\mathbb{1}(c_i \in M_1)}{\sum_{i=1}^m \gamma_{i,n}k(x, c_i)}.$$

The goal is to show that computing the voltage function v using α -covers converges towards the same limit object as computing v using a direct sample. To achieve this, the idea is to show that the operators, $A_{\mathcal{C},n}$ and A_n (along with the functions $b_{\mathcal{C},n}, b_n$) behave similarly.

Lemma D.3. Let \mathcal{C} be any α -cover. There exists a function Δ_1 such that the following two things hold. First, for any $v : M \rightarrow [0, 1]$, and any $x \in M$,

$$|(A_{\mathcal{C},n}v)(x) - (A_nv)(x)| < \Delta_1(\alpha), \quad |b_{\mathcal{C},n}(x) - b_n(x)| < \Delta_1(\alpha).$$

Second, $\lim_{\alpha \rightarrow 0} \Delta_1(\alpha) = 0$.

Proof. This directly follows from the fact that k is μ continuous. Since the diameter of each cell is at most α , and since the support of M is compact, we see that the maximum deviation made in a single entry in the corresponding matrices for $A_{\mathcal{C},n}$ and A_n is bounded by some continuous function of α . \square

Lemma D.4. There exists a function $\Delta : \mathbb{R}^+ \rightarrow \mathbb{R}^+$ such that the following hold. First, for any ϵ, δ and α -cover, \mathcal{C} , there exists N such that for all $n \geq N$, with probability at least $1 - \delta$ over $S \sim \mu^n$,

$$|v_n(x) - v_n^{\mathcal{C}}(x)| \leq \Delta(\alpha) + \epsilon.$$

Second, $\lim_{\alpha \rightarrow 0} \Delta(\alpha) = 0$.

Proof. Let m, p, N be such that for all $n \geq N$, $\|A_n^m\|_{\infty} \leq 1 - p$ with probability at least $1 - \delta$ over $S \sim \mu^n$. Such N must exist by Lemma C.7. It follows that with probability at least $1 - \delta$, T_n^m is a nice operator (Definition B.3).

By the definitions of v_n and $v_n^{\mathcal{C}}$, we have that $T_n^m v_n = v_n$ and $T_n^m v_n^{\mathcal{C}} = v_n^{\mathcal{C}}$, where $T_{n,\mathcal{C}}(v) = A_{n,\mathcal{C}}(v) + b_{n,\mathcal{C}}$. It follows by applying the previous lemma m times that

$$|T_n^m(v_n^{\mathcal{C}}) - v_n^{\mathcal{C}}| = |T_n^m(v_n^{\mathcal{C}}) - T_{n,\mathcal{C}}^m(v_n^{\mathcal{C}})| \leq O(m\Delta_1(\alpha)).$$

Since T_n^m is nice with norm at most $1 - p$, it follows by Lemma B.5 that

$$|v_n^{\mathcal{C}} - v_n| \leq O\left(m \frac{\Delta_1(\alpha)}{p}\right).$$

Since m and p can be chosen to be fixed and since $\lim_{\alpha \rightarrow \infty} \Delta_1(\alpha) \rightarrow 0$ from Lemma D.3, it follows that $\Delta(\alpha) \mapsto m \frac{\Delta_1(\alpha)}{p}$ satisfies both properties above which completes the proof. \square

Lemma D.5. *The sequence $v_i^{\mathcal{C}}(x)$ converges in probability.*

Proof. Let the operator $A_{\mathcal{C}}$ and the map $b_{\mathcal{C}}$ be defined as

$$(A_{\mathcal{C}}v)(x) = \frac{\sum_{i=1}^m k(x, c_i) v(c_i) \gamma_i \mathbb{1}(c_i \in M \setminus (M_0 \cup M_1))}{\sum_{i=1}^m \gamma_i k(x, c_i)},$$

and

$$b_{\mathcal{C}}(x) = \frac{\sum_{i=1}^m \gamma_i k(x, c_i) \mathbb{1}(c_i \in M_1)}{\sum_{i=1}^m \gamma_i k(x, c_i)}.$$

Here, we let γ_i denote the probability mass under μ of the cell corresponding to c_i (Note the difference with $\gamma_{i,n}$ defined in Definition D.2). Then by applying an proof analogous to that in Lemma C.8, we have that

$$\Pr_{S \sim \mu^n} [|(A_{\mathcal{C}}v + b_{\mathcal{C}})(x) - (A_{n,\mathcal{C}}u + b_{n,\mathcal{C}}) > \epsilon] < 4 \exp(-Cn\epsilon^2).$$

Applying an argument analogous to that in Lemma C.9 finishes the proof. \square

Finally, Theorem 6.8 is a direct consequence of the previous two lemmas.

E Properties of the region-based effective resistance

E.1 The reduced graph

[15] offer an interpretation of the effective resistance between sets X_a, X_b on a graph G as the effective resistance between two aggregated nodes a, b on a reduced graph G_{ab} . We extend the concept of a reduced graph to more than two nodes by considering the reduced graph corresponding to the sets X_a, X_b, X_z .

We define $P_{abz} = [\mathbb{1}_n(X_a) \ \mathbb{1}_n(X_b) \ \mathbb{1}_n(X_z) \ I_c] \in \mathbb{R}^{n \times (c+3)}$, where $\mathbb{1}_n(X_p) \in \mathbb{R}^n$ is the indicator vector

$$\mathbb{1}_n(X_p) = \begin{cases} 1, & \forall i \in X_p \\ 0, & \text{otherwise} \end{cases} \quad (\text{E.1})$$

and $I_c \in \mathbb{R}^{n \times c}$ is the matrix collecting all basis vectors e_i for $i \in X_c$.

Definition E.1. (*Reduced graph*) We define the reduced graph of G , with respect to the non-empty disjoint subsets $X_a, X_b, X_z \subset X$, to be the graph G_{abz} with Laplacian $L_{G_{abz}} := P_{abz}^\top L_G P_{abz}$.

The relation between the reduced graph G_{abz} and G is given by Lemma E.2. We note that the interpretation offered by Lemma E.2 will be used in our experiments presented in Section 7, where the degree of the source and sink sets will be taken as the degree of the corresponding aggregated nodes.

Lemma E.2. *The reduced graph G_{abz} corresponds to reducing the nodes in G contained in each of the subsets X_p for $p \in \{a, b, z\}$ into corresponding aggregated nodes a, b , and z that satisfy the following properties for each aggregated node.*

- The degree D_p of each aggregated node p is $D_p = \sum_{i \in X_p} D_i - \sum_{i \in X_p} \sum_{j \in X_p, j \neq i} W_{ij}$
- All external edges from each of the sets X_p to the complement $X \setminus X_p$ are preserved such that

- The edge weights of each aggregated node p to a node $i \in X_c$ are given by $W_{pi} = \sum_{j \in X_p} W_{ji}$
- The edge weights of each aggregated node p to another aggregated node $q \neq p$ is $\sum_{j \in X_p} \sum_{j \in X_q} W_{ji}$

Proof. We write $L_G P_{abz}$ in block form $L_G P_{abz} = [L\mathbb{1}_n(X_a) \quad L\mathbb{1}_n(X_b) \quad L\mathbb{1}_n(X_z) \quad LI_c] \in \mathbb{R}^{n \times (c+3)}$. This gives

$$L_{G_{abz}} = P_{abz}^\top L_G P_{abz} = \begin{bmatrix} L_{aa} & L_{ab} & L_{az} & L_{ac} \\ L_{ba} & L_{bb} & L_{bz} & L_{bc} \\ L_{za} & L_{zb} & L_{zz} & L_{zc} \\ \hline L_{ca} & L_{cb} & L_{cz} & L_{cc} \end{bmatrix}$$

where $L_{pq} = \sum_{i \in X_p} \sum_{j \in X_q} (L_G)_{ij}$ for $p, q \in \{a, b, z\}$, $L_{cq}(i) = \sum_{j \in X_q} (L_G)_{ij}$ for $i = 1, \dots, c$ and $L_{cc} \in \mathbb{R}^{c \times c}$ is the Laplacian on X_c . Now $(L_G)_{ij} = -W_{ij}$ for $i \neq j$, where W_{ij} is the edge weight between node i, j , and $L_{ij} = D_i$ for $i = j$, where D_i is the degree of node i . The interpretation of the blocks follows. \square

Lemma E.3. *The effective resistance between the nodes $p, q \in \{a, b, z\}$ in the graph G_{abz} corresponds to the effective resistance between the corresponding non-empty disjoint sets X_p, X_q in the graph G such that $R_{G_{abz}}(p, q) = R_G^s(X_p, X_q)$.*

Proof. From Theorem E.5, Definition E.1 and Lemma E.2 it follows that

$$R_G^s(X_a, X_b) = (e_1 - e_2)^\top (P_{abz}^\top L_G P_{abz})^\dagger (e_1 - e_2) = (e_1 - e_2)^\top (L_{G_{abz}})^\dagger (e_1 - e_2) = R_{G_{abz}}(p, q).$$

\square

E.2 Proof of Theorem 5.1 Triangle inequality for ER between sets

Consider the setting in Section 2.2. The effective resistance between sets can be calculated using the voltage difference formulation of Proposition 2.3, by extending the source and sink constraints to the subsets. We require $\sum_{i \in X_s} J_i = 1$ and similarly $\sum_{i \in X_g} J_i = -1$. With $J_i = (Lv)_i$ from Eq. (2.3) we have $\sum_{i \in X_s} (Lv)_i = 1$ and $\sum_{i \in X_g} (Lv)_i = -1$. Proposition E.4 defines the new optimization problem we need to solve.

Proposition E.4 (Voltage difference formulation on sets). *The effective resistance between the non-empty disjoint subsets $X_s, X_g \subset X$ corresponds to $R^s(X_s, X_g) = E(\nu)$, where ν is the voltage that minimizes the energy*

$$\begin{aligned} \min_{\nu} \quad & \sum_{x_i, x_j \in X} W_{i,j} (v(x_i) - v(x_j))^2 \\ \text{Subject to} \quad & \sum_{i \in X_s} (Lv)_i = 1, \quad \sum_{i \in X_g} (Lv)_i = -1, \quad (Lv)_i = 0, \forall i \in X_c \end{aligned}$$

Proof. Theorem 2 in [15]. \square

The next theorem extend the result in Theorem 2, Song et al. [15] to an additional subset $X_z \subset X$. Where X_z is non-empty and disjoint from X_a, X_b .

Theorem E.5. *The effective resistance from Proposition E.4 can be written as*

$$R_G^s(X_a, X_b) = (e_1 - e_2)^\top (P_{abz}^\top L_G P_{abz})^\dagger (e_1 - e_2)$$

where $e_i \in \mathbb{R}^{c+3}$ is a basis vector with 1 at i and zero otherwise.

Proof. Using P_{abz} , we can write the constraints in Proposition E.4 in a more compact form $P_{abz}^\top L = (e_1 - e_2)$. Applying these constraints with the Lagrange multiplier $\gamma \in \mathbb{R}^{c+3}$ we have

$$f(v, \gamma) = v^\top Lv + \gamma(P_{abz}^\top L - e_1 + e_2)$$

Since the optimization problem is convex, the effective resistance can be found by solving

$$R_G^s(X_a, X_b) = \min_v \max_\gamma f(v, \gamma)$$

The remaining steps can be found in the proof of Theorem 2, Song et al. [15]. \square

Having established the setting, we can move on to the main proof.

Proof. Consider the reduced graph G_{abz} of G from Definition E.1. In this reduced graph the current is injected into the nodes aggregated in a and is extracted from the nodes aggregated in b . We denote the total current y_{ab} . From the conservation of current, we must have that the current y_{ak} and y_{bk} through any internal node $k \in X_c \cup \{z\}$ must satisfy $y_{ab} \geq y_{ak}$ and $y_{ab} \geq y_{bk}$. Let $v(i)$ be the voltage at node i . For the current to flow from a to b , we need the voltage at the nodes to satisfy $v(a) > v(k) > v(b)$ for all $i \in X_c \cup \{z\}$.

The effective resistance of the graph G_{abz} is an intrinsic property of the graph and does not depend on the choice of source and sink. We let a be the source and b the sink. We then have

$$y_{ab} = \frac{v(a) - v(b)}{R_{G_{abz}}(a, b)} \geq \frac{v(a) - v(z)}{R_{G_{abz}}(a, b)} \geq y_{az} \quad \text{and} \quad y_{ab} = \frac{v(a) - v(b)}{R_{G_{abz}}(a, b)} \geq \frac{v(z) - v(b)}{R_{G_{abz}}(a, b)} \geq y_{bz}$$

This gives

$$\frac{v(a) - v(z)}{v(a) - v(b)} \leq \frac{R_{G_{abz}}(a, z)}{R_{G_{abz}}(a, b)} \quad \text{and} \quad \frac{v(z) - v(b)}{v(a) - v(b)} \leq \frac{R_{G_{abz}}(b, z)}{R_{G_{abz}}(a, b)}$$

Adding the two inequalities gives

$$R_{G_{abz}}(a, b) \leq R_{G_{abz}}(a, z) + R_{G_{abz}}(z, b)$$

Using Lemma E.3 we have that $R_{G_{abz}}(p, q) = R_G^s(X_p, X_q)$ for $p, q \in \{a, b, z\}$. The result follows. \square